

Seasonality adaptation patterns of the natural *Arabidopsis* leaf microbiome over several plant generations are shaped by environmental factors

Maryam Mahmoudi¹, Juliana Almario², Katrina Lutap¹, Kay Nieselt³ and Eric Kemen¹

¹Microbial Interactions in Plant Ecosystems, IMIT/ZMBP, Eberhard Karls University of Tübingen, Auf der Morgenstelle 32, 72076 Tübingen, Germany

²Université Claude Bernard Lyon 1, CNRS, INRA, VetAgro Sup, UMR5557 Ecologie Microbienne, F-69622 Villeurbanne, France

³Institute for Bioinformatics and Medical Informatics, Eberhard Karls University of Tübingen, Sand 14, 72076, Tübingen, Germany

Corresponding author:

Eric Kemen

eric.kemen@uni-tuebingen.de

Current address: Microbial Interactions in Plant Ecosystems, IMIT/ZMBP, Eberhard Karls University of Tübingen, Auf der Morgenstelle 32, 72076 Tübingen, Germany

Abstract

The leaf-associated microbiome plays a crucial role in plant health and persistence to biotic and abiotic perturbations. However, factors that drive long-term seasonal adaptations of the leaf microbiome, particularly in response to combined stresses, are not well understood. To investigate seasonal adaptation of the leaf microbiome over five years, we analyzed changes in bacterial, fungal and general eukaryotic communities in and on *Arabidopsis thaliana* leaves from natural populations using molecular markers. We collected samples during spring and fall and used linear regression models and co-occurrence networks to examine the roles of abiotic perturbations, space, and time in shaping the microbiome. Consistent with previous studies, time, space, and host compartment explained more than 18% of microbial community variation. Moreover, we dissect environmental factors that significantly impact microbial community variation. Additionally, we explored the effects of diversity and environmental factors on microbial network complexity and found that decreased diversity was correlated with increased complexity of microbial networks over growing seasons. We were thus able to identify individual microbial taxa that are adapted to specific seasons and their response to abiotic perturbations. We conclude that seasonality adaptation of leaf microbiota is significantly shaped by three environmental factors: radiation, wind speed and drought. Based on our findings we therefore hypothesize that beside space, time and compartment, diversity and stability of microbe-microbe interactions in the phyllosphere are predominantly shaped by a small set of environmental perturbations. Our findings have

practical implications for the selection and development of field-adapted probiotics for agricultural applications.

Keywords

Leaf microbiome, seasonality, microbial network, environmental factors

Introduction

Leaves are colonized by a variety of microbes from various kingdoms, including bacteria, archaea, fungi, oomycetes, protists, and viruses [1]. Numerous studies have shown that leaf microbiota play a beneficial role in protecting against both biotic and abiotic stressors, ultimately promoting plant growth and fitness [2–6]. To leverage the current understanding of the plant microbiome for biotechnological purposes, such as developing plant-protective probiotics, improving productivity, and drive plant biodiversity, it is essential to identify the key factors that shape the composition of leaf microbiota and modulate complex microbe-microbe interactions [7, 8]. The mechanisms that are essential for community assembly, diversity, and function can be categorized into stochastic and deterministic processes [9]. Stochastic processes, such as birth, death, immigration, speciation, and limited dispersal, shape the microbial community structure [10, 11]. However, these processes are difficult to study due to the challenges associated with defining and measuring stochasticity [12]. The second critical process is deterministic, which includes environmental factors and biotic interactions [9]. Apart from these factors, the microbiome can be impacted by sampling time point, geographical location and host genotype [13]. A comparison of root microbiota in various plants (maize, sorghum, and wheat) revealed that these plants had distinct community compositions. This demonstrates that the host plant genotype can impact the identity of its microbiome [14]. Additionally, it was shown that over the course of developmental stages, the microbiome becomes more tissue-specific [15]. Despite the dynamic nature of the microbiome, most studies focus on spatial snapshots without considering long-term temporal dynamics of microbial assembly. Consequently, our knowledge about the underlying mechanisms and factors driving temporal dynamics remains limited. Utilizing long-term microbiome data can help address fundamental questions regarding microbiome dynamics, such as variations in microbial interactions over time and the stability of the microbiome in response to environmental perturbations, as well as the microbial taxa mediating plant performance under changing environmental conditions. In the analysis of longitudinal microbiome data, a range of computational methods is employed, including microbial network analysis and machine learning algorithms [16–18]. Microbial network analysis facilitates the examination of microbe-microbe interactions, providing insights into co-occurrence patterns [19, 20]. Additionally, machine learning algorithms, such as classification and regression, play a crucial role in identifying the environmental or biological factors associated with diverse bacterial taxa. These algorithms enable predictions regarding outcomes, including the identification of key factors that drive changes in microbiome composition, and the revelation of patterns or trends in microbial community dynamics over time. These outcomes provide valuable insights into the interactions between the microbiome and environmental factors, aiding in the

understanding of microbial response to changing conditions and informing decision-making processes in various fields, including agriculture, biotechnology and ecological management [21–24]. Microbes often interact with each other through various relationships, such as mutualism, antagonism and develop a complex system which can change throughout the growing season of plants [25, 26]. The use of microbial interaction network analysis has been useful in understanding the structure of these interactions. Studies on the temporal dynamics of leaf microbiomes using co-occurrence networks over the growing season of plants have found that, although there is a high level of variability in the leaf microbiome, there are temporal patterns with communities and networks undergoing a stabilization phase of decreased diversity and variability at the beginning of the growing season [27, 28]. A recent study on crop microbiomes found that plant developmental stages had a stronger influence on the microbial diversity, composition, and interkingdom networks in the aerial parts of the plants compared to the soil [29]. The plant microbiome represents an open system susceptible to environmental perturbations, significantly shaping the microbiome of all plant organs, including the phyllosphere. These factors, such as precipitation, temperature and drought significantly affect all microbial communities found in different ecosystems [30, 31]. For example, heat can induce drought tolerance in *Arabidopsis* [32]. In an association analysis between climate data and microbiome composition in *Arabidopsis thaliana* populations, drought was identified as the best predictor of microbiome composition [33]. Drought in turn has been shown to alter the microbial community dynamics in grass root microbiomes [34]. Precipitation on the other hand can determine soil microbial community composition as well [35]. Given that extremes of such factors are becoming more frequent and the average temperature is constantly increasing, the potential impact of warming on the abundance and composition of the phyllosphere microbiome is still understudied [36]. Warming may decrease the presence of beneficial microbes or increase the transmission of pathogens as has been shown for grassland ecosystems [37]. As global climate change leads to a decrease in precipitation and an increase in drought frequency and duration [31], this could have significant impacts on global agricultural production by altering humidity and water availability for plants [38, 39]. Machine learning methods have proven useful in this context, as they have been employed to associate climate data with crop productivity and predict wheat yield throughout the growing season based on climate data [40]. Given such critical conditions for the plants, a stable microbiome might be crucial to increase holobiont (assemblage of a plant and its microbiome living in or around it) plasticity. However, current investigations on the phyllosphere microbiome have primarily focused on bacterial and fungal communities, with limited attention given to other eukaryotes [1], especially in long-term studies. All these observations emphasize the importance of comprehending the potential outcomes of alterations to the phyllosphere microbiome on ecosystem functionality amidst a changing environment [36]. The aim of this study was to analyze long-term temporal dynamics in the leaf microbiome of natural *Arabidopsis thaliana* in response to naturally occurring environmental fluctuations in order to dissect individual biotic and abiotic perturbations affecting community diversity and quantitative composition over time. Amplicon sequencing was used to follow leaf microbial communities with a focus on bacteria, fungi and other eukaryotes over five consecutive years and two seasons. With respect to seasonality, we selected one sampling in fall when plants start their vegetative stage from seedlings before arresting over winter and one sampling in spring when the plants change from vegetative to

reproductive growth (beginning of flowering). Our findings demonstrate that the seasonality patterns of the leaf microbiome are not only influenced by ecological factors (site, season, and compartment), but also shaped by environmental factors. We identified various environmental factors that affect the diversity and abundance of the leaf microbiome. Furthermore, our study showed that the connectivity of microbe-microbe interactions increases during the growing season, while diversity decreases. These changes are significantly associated with environmental factors, indicating the role of abiotic factors in shaping biotic interactions.

Results

Seasonal dynamics of microbial communities in different geographical locations and host compartment

To study the temporal and species dynamics of leaf microbiome, we collected samples from six locations with stable *A.thaliana* populations in the proximity to Tuebingen [27]. Leaf samples were collected over two seasons: in the fall and in the spring. Fall covers the early growth phase of *A. thaliana* under short day conditions before resting in winter. Spring includes samples just before the reproductive stage during increasingly longer days. Sampling was repeated over five consecutive years (Fig. 1; see also Table S1 in the supplemental material). From each sample, we recovered epiphytic and endophytic microbes, extracted genomic DNA, and performed bacterial 16S rRNA, fungal ITS2 and eukaryotic 18S rRNA amplicon sequencing, as described in [27]. To investigate the effect of season, compartment and site on diversity and variation between samples of microbial communities, we conducted multivariate approaches including principal coordinate analysis (PCoA) and permutational multivariate ANOVA (PerMANOVA) on the relative abundance of bacterial, fungal and eukaryotic taxa. The PCoA revealed a clear separation between samples of different seasons and compartments in microbial communities of bacteria, fungi and eukaryotes. Separation among the sites is more pronounced in eukaryotes, followed by fungi and last bacteria (Fig. 2B). PerMANOVA results indicate that season, compartment and site together explain 21.5% variation in bacterial ('season' 3.0%, 'compartment' 8.3% and 'site' 5.3%), 11.8% in fungal ('season' 1.5%, 'compartment' 1.8% and 'site' 4.5%) and 22.4% in eukaryotic ('season' 0.7%, 'compartment' 9.6% and 'site' 6.6%) communities. Furthermore, alpha diversity, as assessed by Shannon's H index, was examined using ANOVA to determine the effects of the different factors on microbial diversity. The results were consistent with previous observations, indicating significant effects of all factors on the diversity of bacteria, fungi, and eukaryotes, except for season in fungi (Table. S2). These diversity patterns were further visualized, showing significant differences between spring and fall samples for bacteria and eukaryotes, while no significant differences were observed for fungi (Fig. S1A). The epiphytic compartment consistently exhibited greater diversity across all microbial communities (Fig. S1B). The impact of the site factor on diversity patterns varied across taxa, with inconsistent effects observed (Fig. S1C). To correlate explained variations among seasons with composition of microbial communities, we compared relative abundance of the microbiome for highly abundant microbes aggregated at the order level between spring and fall samples. In bacteria relative abundance of Sphingomonadales, Propionibacteriales, Micrococcales increased in spring, while Burkholderiales, Enterobacterales, Flavobacteriales

tended to decrease. As for fungi, the relative abundance of Tubeufiales, Tremellales, Leucosporidiales, Helotiales and Cantharellales increased, while that of Pleosporales and Glomerellales decreased. In other eukaryotes Oomycota and Cercozoa_unc increased in spring, while Chlamydomonadales and Vannellida decreased (Fig. S2 and S3).

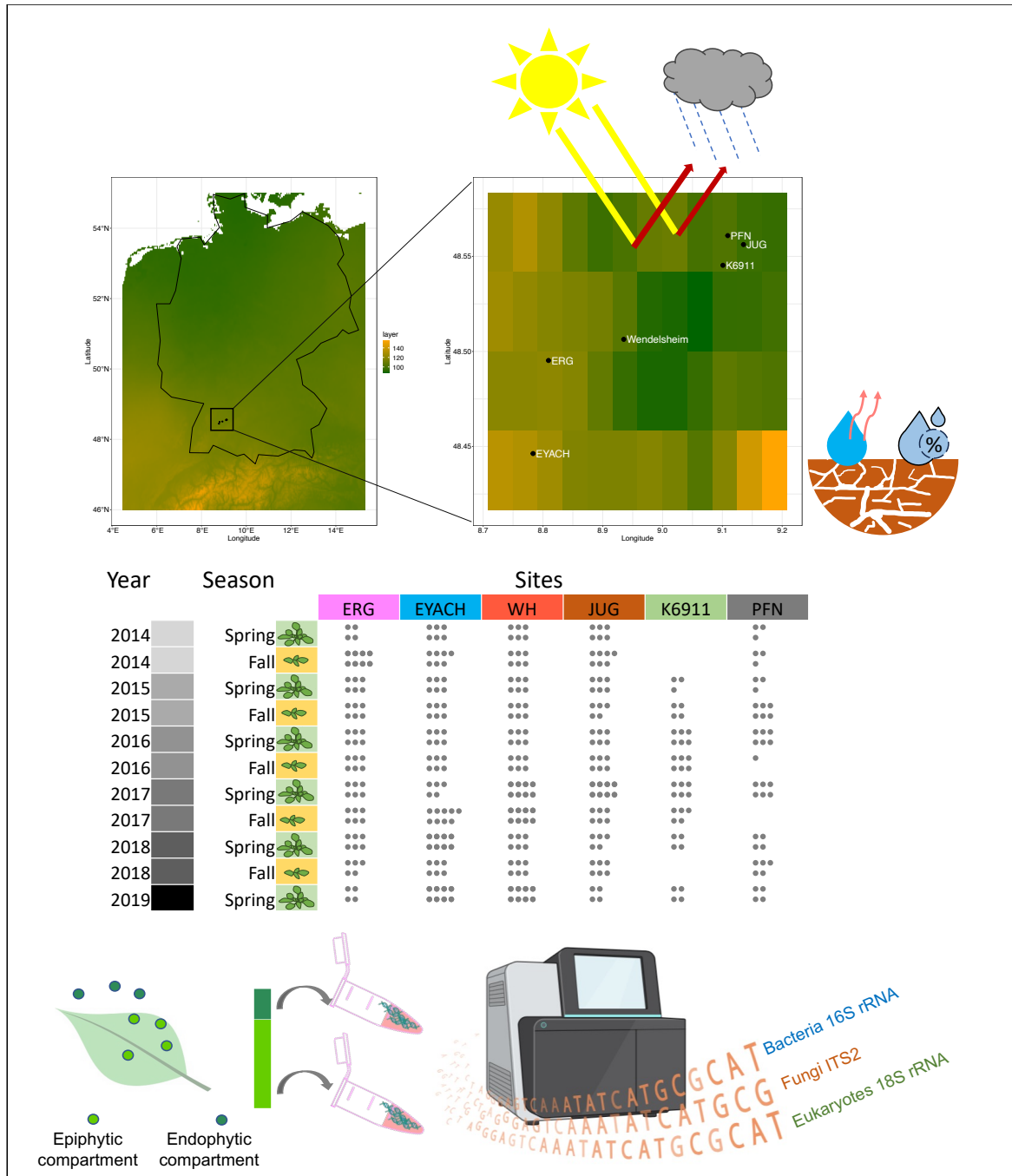


Figure 1. Microbial community collection in natural *A. thaliana* populations over time. Map showing the six sampling locations of natural *A. thaliana* in southern Germany near Tuebingen [27]. Heatmap of the map shows the spatial radiations. Plants were collected in fall and spring of five consecutive years (start spring 2014 to spring 2019, eleven time points, dots represent the sampled plants). Leaf samples were taken for microbiome analysis of epiphytic and endophytic compartments with a total number of 703 samples (see Table. S1). Microbiome analysis was conducted via Illumina-based

amplicon sequencing (Miseq 2x300 cycle). Environmental variables (Table. S3) used in this study were obtained from the TerraClimate [71] database.

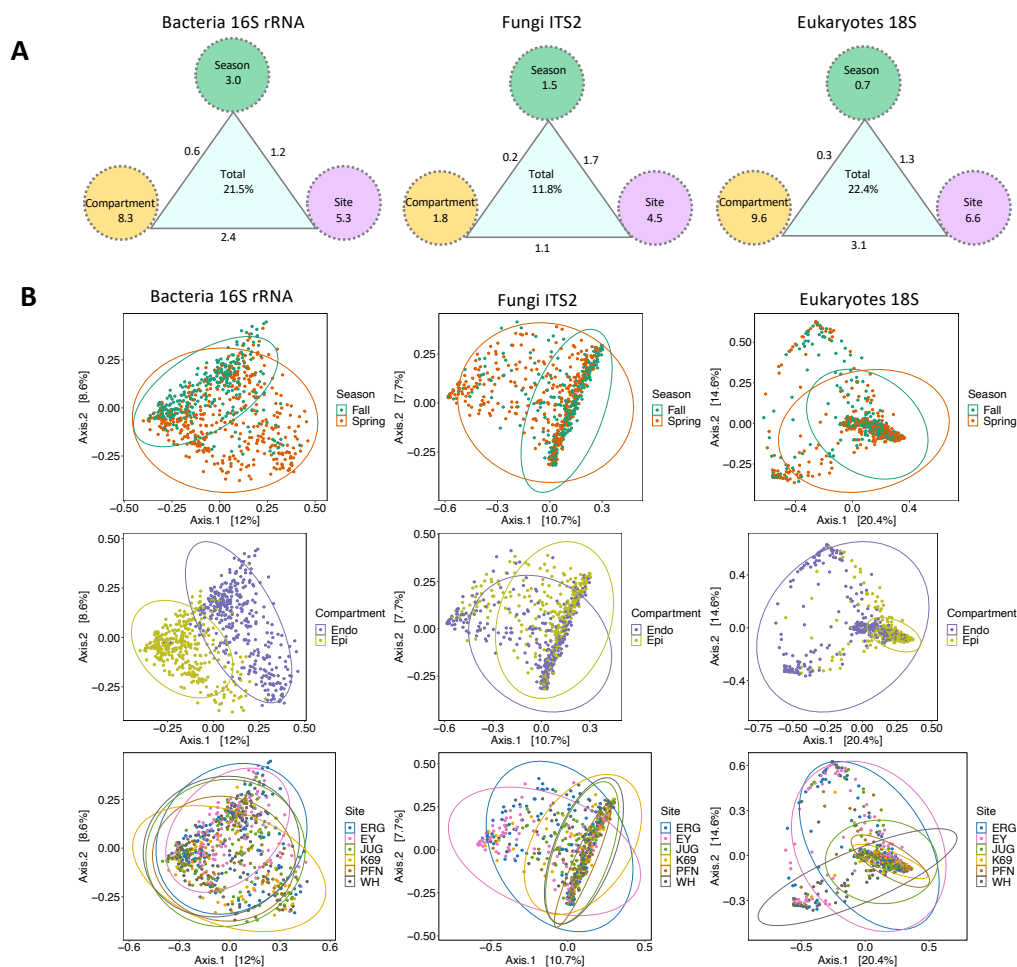


Figure 2. Multivariate analysis on factors structuring leaf microbial communities. (A) A PerMANOVA analysis on Bray-Curtis distances was conducted using the Adonis2 function in Vegan. Circles depict the percentage of variance explained by factors 'season', 'compartment' and 'site', connecting lines depict the percentage of variance explained by interactions between factors. Only significant effects are shown (permutations 10,000, $P < 0.05$, explanatory categorical variables: Season x Compartment x Site). (B) Principal coordinates analysis of epiphytic and endophytic samples of different seasons and sites, measured by principal Bray-Curtis distances in bacterial, fungal and eukaryotes communities.

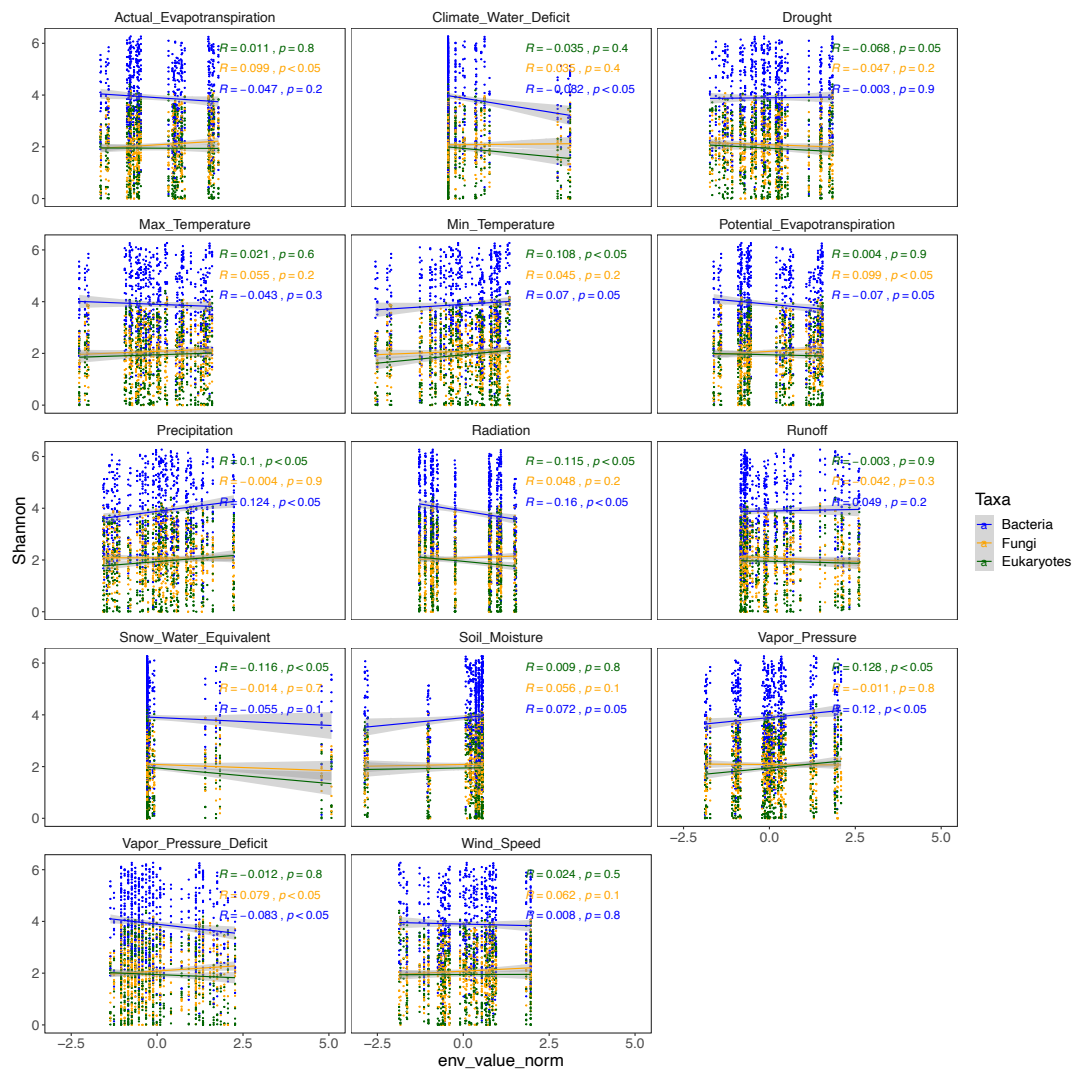


Figure 3. The relationship between alpha diversity (as measured by Shannon's H index) and various environmental factors. Each plot shows a linear regression model fit to the data, with individual samples represented by dots. The bacterial community is represented in blue, the fungal community in orange, and other eukaryote communities in a different color. Grey lines indicate 95% confidence intervals, and the Spearman correlation coefficient (R) and significant correlations ($P < 0.05$) are also shown.

Environmental factors shaping the diversity of leaf microbial communities.

To investigate the factors driving seasonal shifts in the leaf microbiome, we hypothesized that environmental factors are playing a deterministic role. We compared fourteen environmental factors (listed in Table. S3) across the sampling months and sites between spring and fall and found significant differences for all factors except four factors (Fig. S4). Multivariate analyses showed a significant contribution of all environmental factors (15.65% in bacteria, 11.5% in fungi and 8.87% in eukaryotes communities, Table S4). Of the environmental factors, radiation, wind speed and drought were the three most important factors influencing community variation (2.45% in bacteria, 1.32% fungi, and 1.23% in eukaryotes. Fig. 4). Furthermore, to visualize the relationships between environmental factors and community composition, we employed canonical correspondence analysis (CCA, Fig. S5). The CCA results reinforced the findings from the multivariate analyses and revealed

strong correlations between these factors and community composition. Notably, radiation exhibited the highest correlation with CCA2 in bacteria ($R=-0.72$, Fig. S7), while wind speed in fungi ($R=0.53$, Fig. S6) and drought in eukaryotes ($R=-0.35$, Fig. S6) were identified as the most correlated factors with CCA1. We also found a significant correlation between environmental factors and alpha-diversity. Specifically, radiation was positively correlated with alpha-diversity in bacteria ($R=0.15$), evapotranspiration was positively correlated with alpha-diversity in fungi ($R=0.09$), and for eukaryotes, vapor pressure correlated with alpha-diversity ($R=0.12$) (Fig. 3).

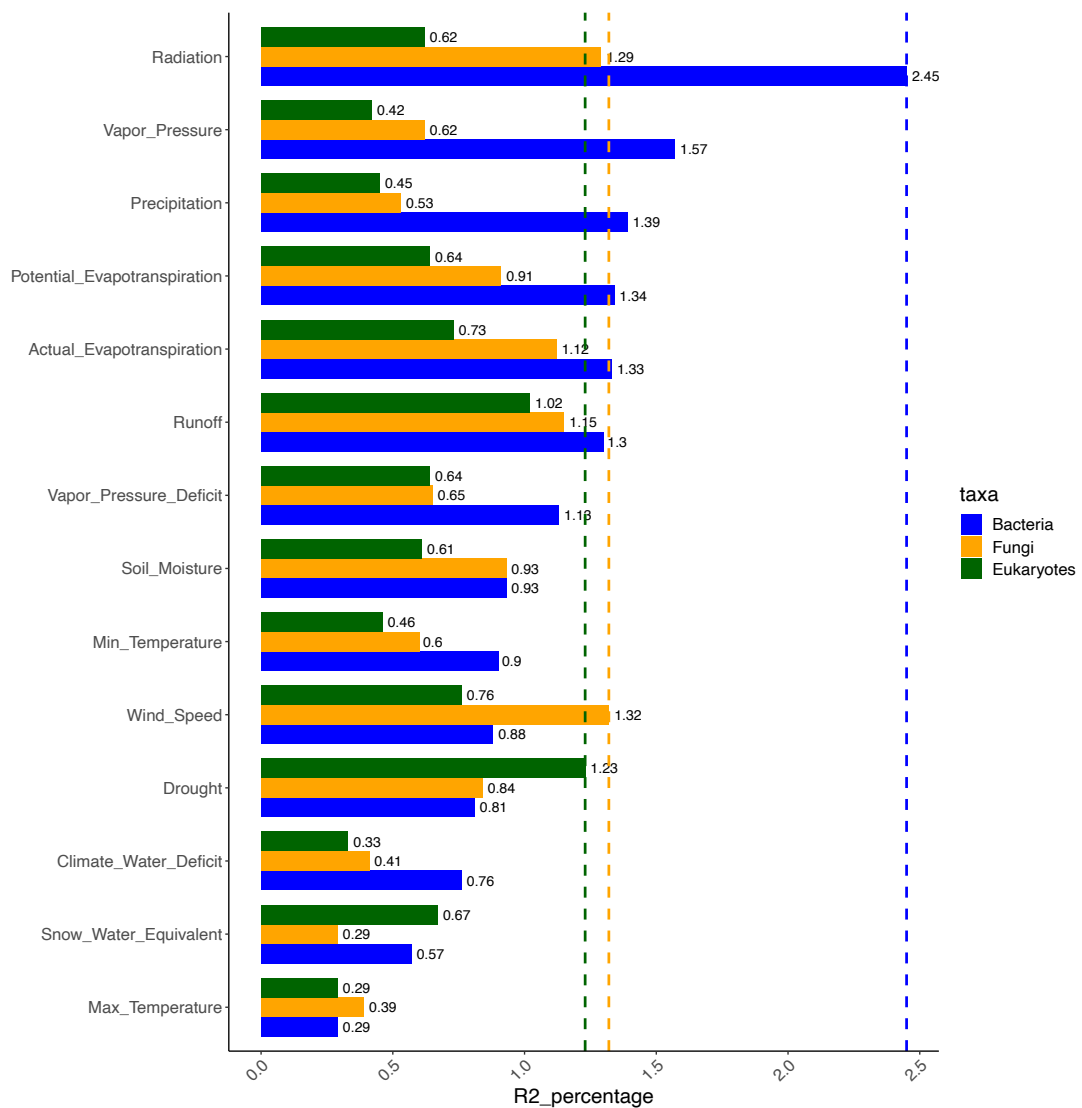


Figure 4. Permutation analysis of variance (PERMANOVA) to investigate the impact of environmental factors on the structure of leaf microbial communities. The analysis was performed using the Adonis2 function in the Vegan package, based on Bray-Curtis distances. The bar plots show the percentage of variance explained by each factor for the bacterial (blue), fungal (orange), and eukaryotes (green) communities. The highest level of explained variation for each microbial group is indicated by a vertical line.

Composition of the leaf microbiome is predictable by environmental factors.

To examine whether environmental factors are associated with relative abundance of microbial communities (bacteria, fungi and eukaryotes), we employed a linear regression model. This model utilized environmental factors as independent variables to predict the aggregated relative abundances at the genus level. By calculating the average coefficient value for each environmental factor, we were able to determine the respective impact of these factors in predicting the relative abundance of microbial taxa. The results show that the factors max-temperature for bacterial and eukaryotes and radiation for fungal communities are the most important in predicting relative abundances of most genera (80% of the bacterial genus, 59% fungi and 71% in other-eukaryotes) (Fig. 5A). In bacteria *Methylobacterium* increases and *Oxalobacteraceae* decreases with max-temperature, in fungi *Titaea* increases and *Cladosporium* decreases and in eukaryotes *Albugo* increases and *Oomycetes* decreases with max-temperature (Fig. 5C). The results of the linear regression model for the effects of environmental factors on microbiome data were visualized as a network (Fig. 5C), with the nodes representing the microbes and environmental factors and the edges representing the coefficients of the linear model (positive and negative interactions according to coefficient values of the regression model, Fig. 5B).

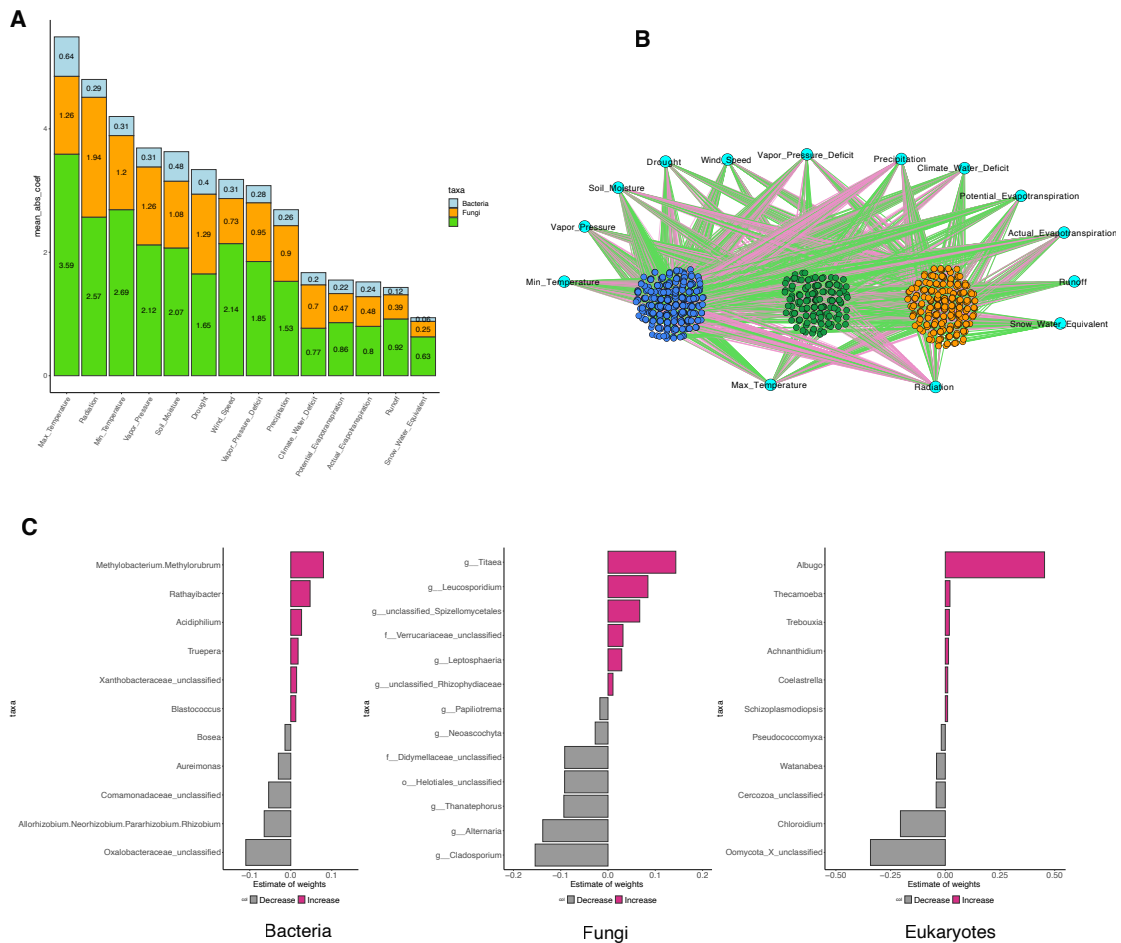


Figure 5. Demonstrates how environmental factors can predict the relative abundance of microbiome taxa. (A) The histograms in the figure represent the average of the absolute coefficient values of each environmental factor that significantly ($p < 0.05$) predicts the relative abundances of bacteria (blue), fungi (orange), and other eukaryotes (green). (B) In the figure, a network of interactions between environmental factors and the microbiome is also shown. The nodes (dots) represent environmental factors or microbes, and the edges (colored lines) depict potential positive and negative coefficient values from the linear regression model. (C) The histograms represent the coefficient values (absolute values ≥ 0.01) calculated using the linear regression model at the genus level for differentially abundant microbes according to maximum temperature in bacteria and eukaryotes, and radiation in fungi. Negative coefficient values (gray bars) represent genera that decrease with these environmental factors, while positive values (pink bars) indicate genera that increase with these factors.

The stability of microbe-microbe interaction networks in response to environmental factors over seasons.

To investigate if observed associations between microbial diversity and environmental factors are correlated with microbe-microbe interactions in different seasons, we used microbial network analysis. We constructed microbial networks for every sampling time point (11) and compared Spring vs Fall networks (Fig. 6A). The SparCC [30] algorithm which is known to be robust for sparse data was used for correlation calculation implemented in FastSpar [31]. Network size (the number of nodes (OTUs) and the number of edges

(correlations between taxa; syn. Connections)) shows that, on average, spring has more edges compared to fall (Fig. 6B). We calculated the cohesion which quantifies the connectivity of the microbe-microbe interaction network. Positive and negative cohesions per sample measured by multiplying relative abundance of OTUs to average of positive and negative correlations respectively. First, we compared the cohesions (positive and negative) over seasons. The results show that in spring there are higher levels of cohesion compared to fall (Fig. 6C and Fig. S8). We measured the association of cohesion with alpha-diversity and results show that cohesion (positive and negative) negatively associates with alpha diversity in both seasons (Fig. 6D). A similar trend was observed for correlation between within-season variability (sample distance to the seasons centroid) and positive cohesion, but the significance was only observed for the spring season. Furthermore, within-sample variability exhibited a positive correlation with negative cohesion (Fig. 6E). As we observed before, diversity is affected by environmental factors and is associated with connectivity of the network. Next, to see if connectivity of the networks is associated with environmental factors, we correlated environmental factors with network cohesion (positive and negative). According to the findings, positive cohesion has a strong association with nine environmental factors, with radiation having the highest positive correlation and vapor pressure having the highest negative correlation with positive cohesion (Fig. S9). Negative cohesion also displays a significant correlation with eight environmental factors (as shown in Fig. S10), with radiation having the highest positive correlation and vapor pressure having the highest negative correlation.

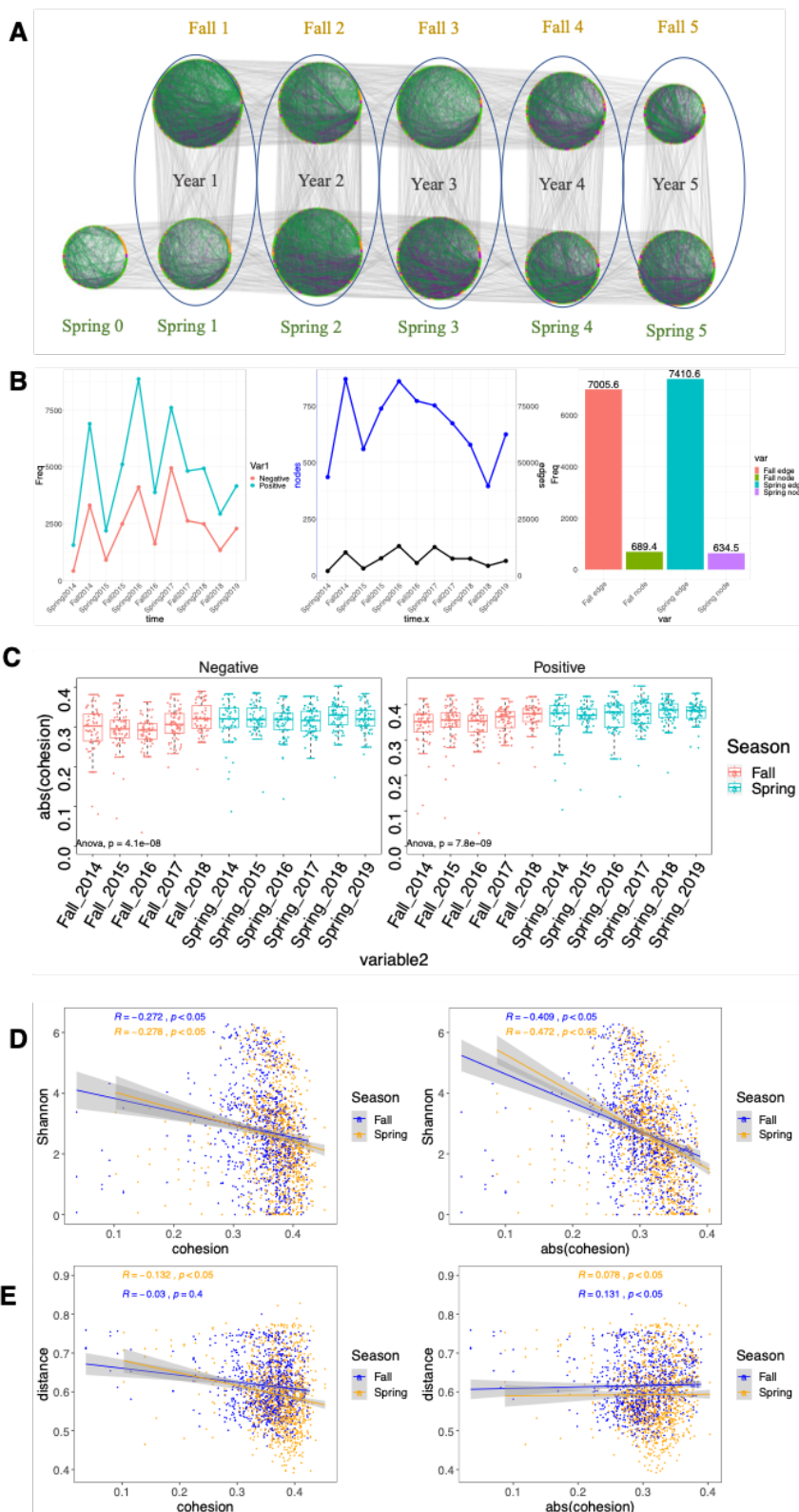


Figure 6. Changes in microbial interaction networks throughout the growing season of *A. thaliana* over multiple years. (A) Data from each time point was used to reconstruct co-abundance networks for each season using the SparCC algorithm. The nodes (dots) represent OTUs, and the edges (colored lines) depict potential positive and negative interactions between OTUs (connections). Gray lines connecting the networks show nodes that are conserved in networks from one time point to the next (inherited nodes). (B) Shows the number of nodes and edges in each time point and then the averages

per season. (C) Box plots represent the negative and positive cohesions in each time point. (D) Shows the correlation between positive and negative cohesions with alpha-diversity (as measured by Shannon's H index) over seasons. (E) Shows the correlation between positive and negative cohesions and within-season variability (distance to the group centroid; beta-dispersion) over seasons. The grey lines indicate 95% confidence intervals, and the Spearman correlation coefficient (R) and significant correlations ($P < 0.05$) are also shown. Individual samples are represented by dots.

Discussion

The leaf microbiome is a dynamic and complex ecosystem that changes its structure in response to various ecological and abiotic factors. Geographical locations, plant compartment and growing season are among the main ecological factors that shape the microbial communities in natural plants. Despite some research has been conducted on the impact of geographical locations, compartment and short period of time on the formation of microbial communities in natural plants [13, 41–44], there is still a lack of studies exploring the role of abiotic factors in shaping microbial communities throughout the plants growing seasons over several plant generations. A further question not studied so far is to what extent does the stability of biotic interaction networks are susceptible to abiotic factors? To address these fundamental ecological questions, we conducted a five-year study on the leaf microbiome of *Arabidopsis thaliana* from natural populations in six geographical locations in the region of Tuebingen Germany [27]. Our findings showed that plant compartment, season, and geographical location significantly impact the microbial communities, explaining 12-22% of their variability (including bacteria, fungi, and other eukaryotes) (Fig. 2A). These results are consistent with previous studies on the variation of microbial communities in different plant compartments and growing seasons [13, 24, 38–41]. The surge in microbial time series investigations provides novel understandings of the stability and dynamics of microbial communities [17]. It's important to note that temporal variations are not limited to global diversity, as evidenced by long-term marine microbiota studies that have uncovered compelling seasonal patterns in the behavior of individual community constituents, among other revelations [45]. It has been demonstrated that the leaf microbiome of *Arabidopsis thaliana* is highly dynamic during the growing seasons from November to March and exhibits conserved patterns. These dynamic changes are observed in the microbial communities of bacteria, fungi, and oomycetes [28]. In this study we showed, although significant variability was observed between seasons, certain microbial groups displayed differences between seasons. Notably, Sphingomonadales, Pleosporales, and Oomycota showed high seasonal differences and were found to be relevant for plant growth over developmental stages (Fig. S2 and S3). Previous research has shown that species of the Sphingomonadales group promote plant growth by producing essential hormones and protecting the plants from pathogens [4]. The decrease of Sphingomonas in the cold period and increase in the warmer seasons could be explained by the finding that the species of this group promote plant growth by producing essential hormones and protecting the plants

against pathogens that develop with an increase in temperature [46, 47]. Similarly, unknown Pleosporales isolates showed plant growth-promoting ability [48], while the Oomycota group contains many known plant pathogens, such as *Albugo* and *Hyaloperonospora*. This is consistent with the disease patterns of downy mildew in Brassicaceae, which are typically facilitated by cold and damp weather conditions. This observation suggests that the plant experiences higher levels of pathogenic pressure during the early stages of growth, particularly in *Arabidopsis* populations within Germany where the growing season occurs during winter [28]. The results of our study were consistent with this pattern, as we observed an increase in pathogenic microbes (Oomycota) in *Arabidopsis* plants during the warmer season in spring. Therefore, we examined how different environmental factors influence diversity, variation and biotic interaction networks in microbial communities over growing seasons.

Environmental factors positively and negatively correlated with the diversity and variability of the leaf microbiome

In this study, we investigated the impact of environmental factors on the plant microbiome. Our results indicate that the selected environmental factors have a significant effect on the microbial communities associated with the plant. Specifically, we found that radiation has a significant effect on bacterial communities, while wind speed influences fungal communities. On the other hand, eukaryotic communities are strongly influenced by drought (Fig. 4). Plants have evolved functional strategies to cope with environmental stressors, and this is reflected in the composition of their microbiome. For instance, bacteria in the plant microbiome produce pigments that protect against reactive oxygen species (ROS), a defense mechanism that is particularly important in the presence of high levels of UV radiation [5, 49]. Additionally, biofilms may also play a role in protecting microorganisms against UV radiation [50]. Furthermore, existing studies have characterized that wind can facilitate the spread of fungal diseases through the dispersal of microscopic spores among crops [51]. Our findings also suggest that the composition of the plant microbiome is strongly influenced by drought-associated metrics, which are known to be a major selective agent on *A. thaliana* populations. The reproducible and predictable associations between specific microbes and water availability suggest that drought not only directly shapes genetic variation in *A. thaliana* but also indirectly through its effects on the leaf microbiome [33]. Moreover, previous studies have reported that drought can have a significant impact on the dynamics of microbial communities in grass root microbiomes [34]. Our modeling analysis revealed that maximum temperature is the main driver of microbial community composition in both bacteria and eukaryotes, while radiation has the strongest influence on fungi communities (Fig. 5A). *Methylobacterium* and *Oxalobacteraceae* groups are highly correlated with maximum temperature in bacteria, while *Albugo* and Oomycota are associated with other eukaryotes. Fungi relative abundances in communities are primarily affected by radiation and are associated with the genera *Titaea* and *Cladosporium* (Fig. 5C). Temperature influences endophytic bacteria composition in above-ground and below-ground organs of *Vitis vinifera*, with seasonal temperature variations having a stronger effect on stem bacteria than root bacteria. This suggests that root environments are more stable [52]. Members of the genus *Methylobacterium* are referred to as pink-pigmented facultative methylotrophs because they produce carotenoids and can grow on one-carbon compounds

such as methanol and methylamine as well as on multi-carbon compounds [53]. Upon plant colonization, these facultative methylophs can benefit from the methanol released by the plant during pectin demethylation [54]. Seasonal variations in temperature, day length, and light intensity have significantly impacted the adaptive differentiation between two populations of *Arabidopsis thaliana* in northern and southern Europe [55]. While studies have shown that stability of plant microbial networks can vary over time, little is known about how the diversity of the microbiome is associated with the stability of microbial networks over the growing season of plants, and how the complexity of microbial networks, including both negative and positive interactions, is associated with environmental factors. Therefore, in this study, we investigated the fundamental question of how microbial networks maintain their ecological stability over the growing season using cohesion, a recently introduced method for measuring the complexity of microbial networks [56].

The complexity of microbial network (internal dynamic) partially increases in response to environmental factors (external dynamic) over growing seasons

The organization of species interaction networks and the processes behind their assembly are fundamental to understanding patterns of biodiversity, community stability, and ecosystem functioning [57]. Correlations in microbial networks can provide insights into the mechanisms underlying these patterns, particularly in response to external perturbations [58, 59]. Positive correlations may result from facilitation mechanisms such as cross-feeding, metabolite exchange, and information exchange, while negative interactions could be due to competition for niche and resources [60, 61]. Under environmental pressure, positive interactions may reflect the functional similarity of the taxa, while negative interactions could represent the taxa with divergent niche requirements [58, 62]. Here, comparing networks between spring and fall reveals that spring networks are more interconnected, with higher numbers of positive and negative interactions (Fig. 6B). Higher complexity, such as larger networks, higher connectivity, and higher connectedness, can render the system more resistant to external perturbations [27]. However, more cohesive and complex communities may also be more susceptible to homogenizing selection, while less complex communities are more susceptible to dispersal [63]. By understanding the relationship between internal dynamics and community structuring processes, we can gain insight into microbial population development in natural systems [58]. Cohesion metrics were used to predict community dynamics, with cohesion being significantly related to the rate of compositional turnover (Bray–Curtis dissimilarity) in microbial communities [56]. We show that cohesion (positive and negative) is negatively correlated with diversity, with fewer variable communities tending to be more interconnected and more stable (Fig. 6D and E). We found that spring networks are more stable than fall networks, likely due to external factors affecting the complexity of the microbial networks. Cohesion (positive and negative) is highly correlated with radiation and vapor pressure, suggesting that increased connectivity in response to radiation may be due to interactions that protect the community (Fig. S9 and S10). Temperature has also been shown to increase the complexity of microbial networks over time [64]. Our results show that vapor pressure and the radiation have the highest association with network cohesiveness (Fig. S9 and S10). Overall, our results suggest that environmental factors have differential effects on microbial interconnectivity in different seasons, highlighting the need to consider seasonality in plant microbiome research.

Conclusions

In this study, we have demonstrated the significant roles of environmental factors in shaping the leaf microbial community over time. Our findings are consistent with previous studies, which suggest that while stochasticity is initially important in shaping the community, later on deterministic processes become dominant (e.g., ref. [65, 66]). Additionally, we have established a link between the dynamics of microbial community networks and the diversity and stability of the communities. Specifically, we found that microbial community interconnectivity is negatively correlated with diversity. Furthermore, we demonstrated that environmental factors, beyond biotic interactions due to microbial function, also influence the interactions among the microbiome. Our study represents a novel approach to exploring time-informed community dynamics in natural host-associated microbiomes. In the long term, this research could facilitate the modeling and prediction of microbial community dynamics over time by taking into account external perturbations. By understanding these processes, we may be able to drive microbial communities towards desired states.

Method

Collection of *Arabidopsis thaliana* samples.

Sample collections of wild *Arabidopsis thaliana* samples were collected from six sites near Tuebingen. In the fall and spring of 2014, 2015, 2016, 2017, 2018 and spring of 2019 (11 time points, Table. S1). Epiphytic and endophytic microorganisms were collected from each leaf sample as described in Aglar et al. [27]. In brief, leaves were washed gently with water for 30 sec, then in 3-5 ml epiphyte wash (0.1% Triton X-100 in 1x TE buffer) for 1 min, epiphytic microorganisms collected by filtering the solution through a 0.2 mm nitrocellulose membrane filter (Whatman, Piscataway, NJ, USA). The filter was placed in a screw-cap tube and frozen in ice. For collecting endophytic fractions, the same leaves were surface sterilized by washing with 80% ethanol for 15 sec followed by 2% bleach (sodium hypochlorite) for 30 sec. Leaves were rinsed three times with sterile autoclaved water for 10 sec and samples were placed in a screw-cap tube and frozen on dry ice. DNA extraction and amplicon sequencing Phenol-chloroform based DNA extraction was performed according to a custom protocol as described in Agler et al. [27]. The extracted DNA was used for two-step PCR amplification of the V5-V7 region of bacterial 16S rRNA (primers 799F/1192R), the ITS2 region of fungi (primers fITS7/ITS4), 18S rRNA region of eukaryotes (primers F1422/R1797). Blocking oligos were used to reduce amplification of plant DNA. Purified PCR products were pooled in equimolar amounts before sequencing in Illumina MiSeq runs (600-cycle) with PhiX control.

Amplicon sequencing data analysis.

Amplicon sequencing data was processed in Mothur (Version=1.42.3) [67] environments described in Almario et al. [28]. Single-end reads were combined to make paired-end reads, and paired reads with less than 5 bases overlap between the forward and reverse reads were removed. Only 100-600 bases long reads were kept. Chimeras were detected using Vsearch in Mothur with more abundant sequences as reference. Cutadapt 2.10 [68] was used to trim adapter sequences from 16S rRNA and 18S reads in case short amplicons were completely sequenced through and again recovered matching pairs and “orphan” reads. For fungal reads, we used ITSx 1.1b [69] to trim reads to only the ITS2 region with defaults except that we preserved sequence headers, checked against fungi, oomycete and plant profiles, allowed single domain matching with an e-value cutoff of 1e-5.0, allowed matching of only one HMM gene profile and turned on saving partial ITS regions. Sequences were clustered into Operational Taxonomic Units (OTUs) at the 97% similarity threshold using the VSEARCH program in Mothur. Individual sequences were taxonomically classified using the rdp classifier method (consensus confidence threshold set to 80, method=wang) and the Silva database (version 138.1) for 16S rRNA data, the UNITE_public database (version 02_02_2019) for fungal ITS2 and the Pr2 (version 4.12.0) for eukaryotes. The PhiX genome was included in each of the databases to improve the detection of remaining PhiX reads. Each OTU was then taxonomically classified (consensus confidence threshold set to 80), OTUs with unknown taxonomy at the kingdom level were removed, as were low abundance OTUs (≤ 50 reads).

Diversity analysis.

Sample alpha-diversity analysis was conducted on OTU abundance tables, using Shannon’s H diversity index (estimate-richness function in phyloseq package in R). Data normality was checked (Shapiro-Wilk’s test) and means were compared using a non-parametric test for two (Wilcoxon Rank Sum and Signed Rank Tests, $P < 0.05$) and multiple groups (Dunn’s test, Bonferroni corrected, $P \text{ adj.} < 0.05$). Beta-diversity analyses were conducted on transformed ($\log_{10}(x + 1)$) relative abundance tables. Bray-Curtis dissimilarities between samples were computed and used for principle coordinate analysis (PCoA, function ‘ordinate’, Phyloseq package) and canonical correspondence analysis (CCA, function ‘cca’, Vegan package). A PerMANOVA analysis on Bray-Curtis dissimilarities was conducted to identify the main factors (season, site, compartment and environmental factors) influencing the structure of the leaf microbiome (‘Adonis2’, Vegan package, 10,000 permutations, $P < 0.05$). All analyses were conducted in R 4.1.2.

Linear model analysis.

The environmental variables used in this study were obtained from TerraClimate [70], a database with monthly temporal resolution and approximately 4 km spatial resolution. The following environmental variables (Table. S3) were included in the analysis: aet, Actual Evapotranspiration, monthly total; def, Climate Water Deficit, monthly total; pet, Potential evapotranspiration, monthly total; ppt, Precipitation, monthly total; q, Runoff, monthly total; soil, Soil Moisture; srad, Downward surface shortwave radiation; swe, Snow water equivalent; tmax, Max Temperature; tmin, Min Temperature; vap, Vapor pressure; ws, Wind speed; vpd, Vapor Pressure Deficit; PDSI, Palmer Drought Severity Index. Association between

independent variables (environmental factors) and different dependent variables (alpha diversity, canonical correspondence, cohesion) were assessed using linear models. The association between the z-transformed environmental factors and the dependent variables was examined by constructing models using the `stat_smooth()` function in R. The models were created with the `lm (y ~ Xi)` notation, where X_i represents each environmental factor individually and y represents the corresponding dependent variable. Additionally, correlations were calculated using the `stat_cor(method='pearson')` function in R. To identify importance of environmental factors in prediction of relative abundance of OTUs aggregate at genus level linear regression was conducted (`statsmodels.api.OLS` packages in python as follow: `statsmodels.api.OLS(yi,X).fit()` in python). Y_i is each time one genus and X is the vector of all environmental factors. The absolute average of significant ($p < 0.05$) coefficients of each environmental factor for all the microbes were calculated to show which environmental factor is associated with the majority of microbiome relative abundances. In this study, the coefficients in the linear regression model represent the strength and direction of the relationship between environmental factors (predictor variables) and the relative abundances of bacteria, fungi, and other eukaryotes (response variables). A positive coefficient indicates a positive relationship, meaning that as the value of the predictor variable increases, the response variable also tends to increase. Conversely, a negative coefficient indicates a negative relationship, where an increase in the predictor variable is associated with a decrease in the response variable.

Microbial network calculations and properties

Bacteria, fungi and eukaryote OTU tables were merged and used for correlations calculation using the SparCC algorithm [71] which relies on Aitchison's log-ratio analysis and is designed to deal with compositional data with high sparsity. OTU tables were filtered to OTUs present in at least 5 samples with > 10 reads per OTU. The filtered OTU tables (OTU raw abundances) were used to calculate SparCC correlation scores (with default parameters) in FastSpar platform [72]. Pseudo P-values were inferred from 1000 bootstraps. Only correlations with $P < 0.001$ and absolute correlation > 0 were kept for further analyses. Cytoscape (version 3.7.1) was used for network visualization. Cohesion measuring the complexity of the network which is associated with number and strength of connections could help to predict the dynamic of community [56]. We calculated cohesion, a method to quantify the connectivity of a community. For each sample (j), two cohesions positive and negative (equation1) were calculated by multiplying OTUs relative abundances to average of the positive or negative correlations of OTUs.

equation1:

$$Cohesion_j = \sum_{i=1}^n RA_i * \overline{cor}_{cor,i}$$

Where RA_i is relative abundance of OTU $_i$ in sample j and $\overline{cor}_{cor,i}$ is average of significant positive (range from 0 to +1) or negative (range from -1 to 0) correlations for OTU $_i$.

Availability of data and material:

Sequencing data are available under NCBI Bioproject PRJNA961058. OTU tables and scripts are available here <https://github.com/IshtarMM/AbioticAraMicrobe>

Competing interests: Authors declare no competing financial interests in relation to the work.

Author Contributions: MM, KN and EK conceived and devised the study. MM, JA and KL performed the experiments. MM and JA analyzed the data. MM, JA, KN and EK contributed to writing and preparation of the manuscript. All authors read and approved the final manuscript.

Acknowledgements: We thank KemenLabSamplingTeam for organizing and participating in several sampling trips and Elke Klenk for helping in MiSeq sequencing preparation. This project has been funded by the European Research Council (ERC) under the DeCoCt research program (grant agreement: ERC-2018-COG 820124), the Cluster of Excellence "Controlling Microbes to Fight Infections" (CMFI; Exc 2124) and the SPP 2125 DECrypT program from the DFG.

References:

1. Sapp M, Ploch S, Fiore-Donno AM, Bonkowski M, Rose LE. Protists are an integral part of the *Arabidopsis thaliana* microbiome. *Environ Microbiol* 2018; **20**: 30–43.
2. Helfrich EJ, Vogel CM, Ueoka R, Schäfer M, Ryffel F, Müller DB, et al. Bipartite interactions, antibiotic production and biosynthetic potential of the *Arabidopsis* leaf microbiome. *Nat Microbiol* 2018; **3**: 909–919.
3. Vorholt JA. Microbial life in the phyllosphere. *Nat Rev Microbiol* 2012; **10**: 828–840.
4. Innerebner G, Knief C, Vorholt JA. Protection of *Arabidopsis thaliana* against leaf-pathogenic *Pseudomonas syringae* by *Sphingomonas* strains in a controlled model system. *Appl Environ Microbiol* 2011; **77**: 3202–3210.
5. Kamo T, Hiradate S, Suzuki K, Fujita I, Yamaki S, Yoneda T, et al. Methylobamine, a UVA-absorbing compound from the plant-associated bacteria *Methylobacterium* sp. *Nat Prod Commun* 2018; **13**: 1934578X1801300208.

6. Ritpitakphong U, Falquet L, Vimoltust A, Berger A, Métraux J-P, L'Haridon F. The microbiome of the leaf surface of *Arabidopsis* protects against a fungal pathogen. *New Phytol* 2016; **210**: 1033–1043.
7. Chaudhry V, Runge P, Sengupta P, Doehlemann G, Parker JE, Kemen E. Shaping the leaf microbiota: plant–microbe–microbe interactions. *J Exp Bot* 2021; **72**: 36–56.
8. Van Der Heijden MG, Klironomos JN, Ursic M, Moutoglis P, Streitwolf-Engel R, Boller T, et al. Mycorrhizal fungal diversity determines plant biodiversity, ecosystem variability and productivity. *Nature* 1998; **396**: 69–72.
9. Yuan H, Mei R, Liao J, Liu W-T. Nexus of stochastic and deterministic processes on microbial community assembly in biological systems. *Front Microbiol* 2019; **10**: 1536.
10. Sloan WT, Lunn M, Woodcock S, Head IM, Nee S, Curtis TP. Quantifying the roles of immigration and chance in shaping prokaryote community structure. *Environ Microbiol* 2006; **8**: 732–740.
11. Chen W, Ren K, Isabwe A, Chen H, Liu M, Yang J. Stochastic processes shape microeukaryotic community assembly in a subtropical river across wet and dry seasons. *Microbiome* 2019; **7**: 1–16.
12. Zhou J, Ning D. Stochastic community assembly: does it matter in microbial ecology? *Microbiol Mol Biol Rev* 2017; **81**: e00002-17.
13. Runge P, Ventura F, Kemen E, Stam R. Distinct phyllosphere microbiome of wild tomato species in central Peru upon dysbiosis. *Microb Ecol* 2023; **85**: 168–183.
14. Bouffaud M-L, Poirier M-A, Muller D, Moënne-Loccoz Y. Root microbiome relates to plant host evolution in maize and other *Poaceae*. *Environ Microbiol* 2014; **16**: 2804–2814.
15. Beilsmith K, Perisin M, Bergelson J. Natural bacterial assemblages in *Arabidopsis thaliana* tissues become more distinguishable and diverse during host development. *Mbio* 2021; **12**: e02723-20.
16. Matchado MS, Lauber M, Reitmeier S, Kacprowski T, Baumbach J, Haller D, et al. Network analysis methods for studying microbial communities: A mini review. *Comput Struct Biotechnol J* 2021; **19**: 2687–2698.

17. Faust K, Lahti L, Gonze D, De Vos WM, Raes J. Metagenomics meets time series analysis: unraveling microbial community dynamics. *Curr Opin Microbiol* 2015; **25**: 56–66.
18. Marcos-Zambrano LJ, Karaduzovic-Hadziabdic K, Loncar Turukalo T, Przymus P, Trajkovic V, Aasmets O, et al. Applications of Machine Learning in Human Microbiome Studies: A Review on Feature Selection, Biomarker Identification, Disease Prediction and Treatment. *Front Microbiol* 2021; **12**: 634511.
19. van der Heijden MGA, Hartmann M. Networking in the Plant Microbiome. *PLOS Biol* 2016; **14**: e1002378.
20. Faust K, Raes J. Microbial interactions: from networks to models. *Nat Rev Microbiol* 2012; **10**: 538–550.
21. Ghannam RB, Techtmann SM. Machine learning applications in microbial ecology, human microbiome studies, and environmental monitoring. *Comput Struct Biotechnol J* 2021; **19**: 1092–1107.
22. Hernández Medina R, Kutuzova S, Nielsen KN, Johansen J, Hansen LH, Nielsen M, et al. Machine learning and deep learning applications in microbiome research. *ISME Commun* 2022; **2**: 98.
23. Namkung J. Machine learning methods for microbiome studies. *J Microbiol* 2020; **58**: 206–216.
24. Xia Y, Sun J. Hypothesis testing and statistical analysis of microbiome. *Genes Dis* 2017; **4**: 138–148.
25. Schlechter RO, Miebach M, Remus-Emsermann MN. Driving factors of epiphytic bacterial communities: a review. *J Adv Res* 2019; **19**: 57–65.
26. Copeland JK, Yuan L, Layeghifard M, Wang PW, Guttman DS. Seasonal community succession of the phyllosphere microbiome. *Mol Plant Microbe Interact* 2015; **28**: 274–285.
27. Agler MT, Ruhe J, Kroll S, Morhenn C, Kim S-T, Weigel D, et al. Microbial hub taxa link host and abiotic factors to plant microbiome variation. *PLoS Biol* 2016; **14**: e1002352.

28. Almario J, Mahmoudi M, Kroll S, Agler M, Placzek A, Mari A, et al. The leaf microbiome of *Arabidopsis* displays reproducible dynamics and patterns throughout the growing season. *Mbio* 2022; **13**: e02825-21.
29. Xiong C, Singh BK, He J-Z, Han Y-L, Li P-P, Wan L-H, et al. Plant developmental stage drives the differentiation in ecological role of the maize microbiome. *Microbiome* 2021; **9**: 1–15.
30. Griffiths RI, Thomson BC, James P, Bell T, Bailey M, Whiteley AS. The bacterial biogeography of British soils. *Environ Microbiol* 2011; **13**: 1642–1654.
31. Sardans J, Peñuelas J, Estiarte M, Prieto P. Warming and drought alter C and N concentration, allocation and accumulation in a Mediterranean shrubland. *Glob Change Biol* 2008; **14**: 2304–2316.
32. Thieme M, Brêchet A, Bourgeois Y, Keller B, Bucher E, Roulin AC. Experimentally heat-induced transposition increases drought tolerance in *Arabidopsis thaliana*. *New Phytol* 2022; **236**: 182–194.
33. Karasov TL, Neumann M, Shirsekar G, Monroe G, PATHODOPSIS Team, Weigel D, et al. Drought selection on *Arabidopsis* populations and their microbiomes. 2022. *Ecology*.
34. Naylor D, DeGraaf S, Purdom E, Coleman-Derr D. Drought and host selection influence bacterial community dynamics in the grass root microbiome. *ISME J* 2017; **11**: 2691–2704.
35. De Vries FT, Manning P, Tallowin JR, Mortimer SR, Pilgrim ES, Harrison KA, et al. Abiotic drivers and plant traits explain landscape-scale patterns in soil microbial communities. *Ecol Lett* 2012; **15**: 1230–1239.
36. Zhu Y-G, Xiong C, Wei Z, Chen Q-L, Ma B, Zhou S-Y-D, et al. Impacts of global change on the phyllosphere microbiome. *New Phytol* 2022.
37. Aydogan EL, Moser G, Müller C, Kämpfer P, Glaeser SP. Long-term warming shifts the composition of bacterial communities in the phyllosphere of *Galium album* in a permanent grassland field-experiment. *Front Microbiol* 2018; **9**: 144.

38. Xu L, Dong Z, Chiniquy D, Pierroz G, Deng S, Gao C, et al. Genome-resolved metagenomics reveals role of iron metabolism in drought-induced rhizosphere microbiome dynamics. *Nat Commun* 2021; **12**: 1–17.
39. Romero F, Cazzato S, Walder F, Vogelgsang S, Bender SF, van der Heijden MG. Humidity and high temperature are important for predicting fungal disease outbreaks worldwide. *New Phytol* 2022; **234**: 1553–1556.
40. Wang Y, Zhang Z, Feng L, Du Q, Runge T. Combining Multi-Source Data and Machine Learning Approaches to Predict Winter Wheat Yield in the Conterminous United States. *Remote Sens* 2020; **12**: 1232.
41. Durán P, Thiergart T, Garrido-Oter R, Agler M, Kemen E, Schulze-Lefert P, et al. Microbial interkingdom interactions in roots promote Arabidopsis survival. *Cell* 2018; **175**: 973–983.
42. Ou T, Xu W, Wang F, Strobel G, Zhou Z, Xiang Z, et al. A microbiome study reveals seasonal variation in endophytic bacteria among different mulberry cultivars. *Comput Struct Biotechnol J* 2019; **17**: 1091–1100.
43. Ware IM, Van Nuland ME, Yang ZK, Schadt CW, Schweitzer JA, Bailey JK. Climate-driven divergence in plant-microbiome interactions generates range-wide variation in bud break phenology. *Commun Biol* 2021; **4**: 748.
44. Edwards J, Johnson C, Santos-Medellín C, Lurie E, Podishetty NK, Bhatnagar S, et al. Structure, variation, and assembly of the root-associated microbiomes of rice. *Proc Natl Acad Sci* 2015; **112**: E911–E920.
45. Giovannoni SJ, Vergin KL. Seasonality in ocean microbial communities. *Science* 2012; **335**: 671–676.
46. Khan AL, Waqas M, Kang S-M, Al-Harrasi A, Hussain J, Al-Rawahi A, et al. Bacterial endophyte *Sphingomonas* sp. LK11 produces gibberellins and IAA and promotes tomato plant growth. *J Microbiol* 2014; **52**: 689–695.

47. Sun M, Chen B, Wang H, Wang N, Ma T, Cui Y, et al. Microbial interactions and roles in soil fertility in seasonal freeze-thaw periods under different straw returning strategies. *Agriculture* 2021; **11**: 779.
48. Ndinga-Muniania C, Mueller RC, Kuske CR, Porras-Alfaro A. Seasonal variation and potential roles of dark septate fungi in an arid grassland. *Mycologia* 2021; **113**: 1181–1198.
49. Ruiz-Pérez CA, Restrepo S, Zambrano MM. Microbial and functional diversity within the phyllosphere of Espeletia species in an Andean high-mountain ecosystem. *Appl Environ Microbiol* 2016; **82**: 1807–1817.
50. Yin W, Wang Y, Liu L, He J. Biofilms: The Microbial “Protective Clothing” in Extreme Environments. *Int J Mol Sci* 2019; **20**: 3423.
51. Mukherjee R, Gruszewski HA, Bilyeu LT, Schmale DG, Boreyko JB. Synergistic dispersal of plant pathogen spores by jumping-droplet condensation and wind. *Proc Natl Acad Sci* 2021; **118**: e2106938118.
52. Campisano A, Albanese D, Yousaf S, Pancher M, Donati C, Pertot I. Temperature drives the assembly of endophytic communities’ seasonal succession. *Environ Microbiol* 2017; **19**: 3353–3364.
53. Green PN. *Methylobacterium*. In: Whitman WB, Rainey F, Kämpfer P, Trujillo M, Chun J, DeVos P, et al. (eds). *Bergey’s Manual of Systematics of Archaea and Bacteria*, 1st ed. 2015. Wiley, pp 1–8.
54. Galbally IE, Kirstine W. The production of methanol by flowering plants and the global cycle of methanol. *J Atmospheric Chem* 2002; **43**: 195–229.
55. Durán P, Ellis TJ, Thiergart T, Ågren J, Hacquard S. Climate drives rhizosphere microbiome variation and divergent selection between geographically distant *Arabidopsis* populations. *New Phytol* 2022; **236**: 608–621.
56. Herren CM, McMahon KD. Cohesion: a method for quantifying the connectivity of microbial communities. *ISME J* 2017; **11**: 2426–2438.

57. Lurgi M, Thomas T, Wemheuer B, Webster NS, Montoya JM. Modularity and predicted functions of the global sponge-microbiome network. *Nat Commun* 2019; **10**: 992.
58. Hernandez DJ, David AS, Menges ES, Searcy CA, Afkhami ME. Environmental stress destabilizes microbial networks. *ISME J* 2021; **15**: 1722–1734.
59. Barberán A, Bates ST, Casamayor EO, Fierer N. Using network analysis to explore co-occurrence patterns in soil microbial communities. *ISME J* 2012; **6**: 343–351.
60. Fuhrman JA. Microbial community structure and its functional implications. *Nature* 2009; **459**: 193–199.
61. Berry D, Widder S. Deciphering microbial interactions and detecting keystone species with co-occurrence networks. *Front Microbiol* 2014; **5**: 219.
62. Chaffron S, Rehrauer H, Pernthaler J, von Mering C. A global network of coexisting microbes from environmental and whole-genome sequence data. *Genome Res* 2010; **20**: 947–959.
63. Danczak RE, Johnston MD, Kenah C, Slattery M, Wilkins MJ. Microbial Community Cohesion Mediates Community Turnover in Unperturbed Aquifers. *mSystems* 2018; **3**: e00066-18.
64. Yuan MM, Guo X, Wu L, Zhang Y, Xiao N, Ning D, et al. Climate warming enhances microbial network complexity and stability. *Nat Clim Change* 2021; **11**: 343–348.
65. Dini-Andreote F, Stegen JC, van Elsas JD, Salles JF. Disentangling mechanisms that mediate the balance between stochastic and deterministic processes in microbial succession. *Proc Natl Acad Sci* 2015; **112**.
66. Bier RL, Vass M, Székely AJ, Langenheder S. Ecosystem size-induced environmental fluctuations affect the temporal dynamics of community assembly mechanisms. *ISME J* 2022; **16**: 2635–2643.
67. Schloss PD. Reintroducing mothur: 10 Years Later. *Appl Environ Microbiol* 2020; **86**: e02343-19.
68. Martin M. Cutadapt removes adapter sequences from high-throughput sequencing reads. *EMBnet.journal* 2011; **17**: 10.
69. Bengtsson-Palme J, Ryberg M, Hartmann M, Branco S, Wang Z, Godhe A, et al. Improved software detection and extraction of ITS1 and ITS2 from ribosomal ITS sequences of fungi and

other eukaryotes for analysis of environmental sequencing data. *Methods Ecol Evol* 2013; n/a-n/a.

70. Abatzoglou JT, Dobrowski SZ, Parks SA, Hegewisch KC. TerraClimate, a high-resolution global dataset of monthly climate and climatic water balance from 1958–2015. *Sci Data* 2018; **5**: 170191.
71. Friedman J, Alm EJ. Inferring correlation networks from genomic survey data. *PLoS Comput Biol* 2012; **8**: e1002687.
72. Watts SC, Ritchie SC, Inouye M, Holt KE. FastSpar: rapid and scalable correlation estimation for compositional data. *Bioinformatics* 2019; **35**: 1064–1066.

Main figures legends

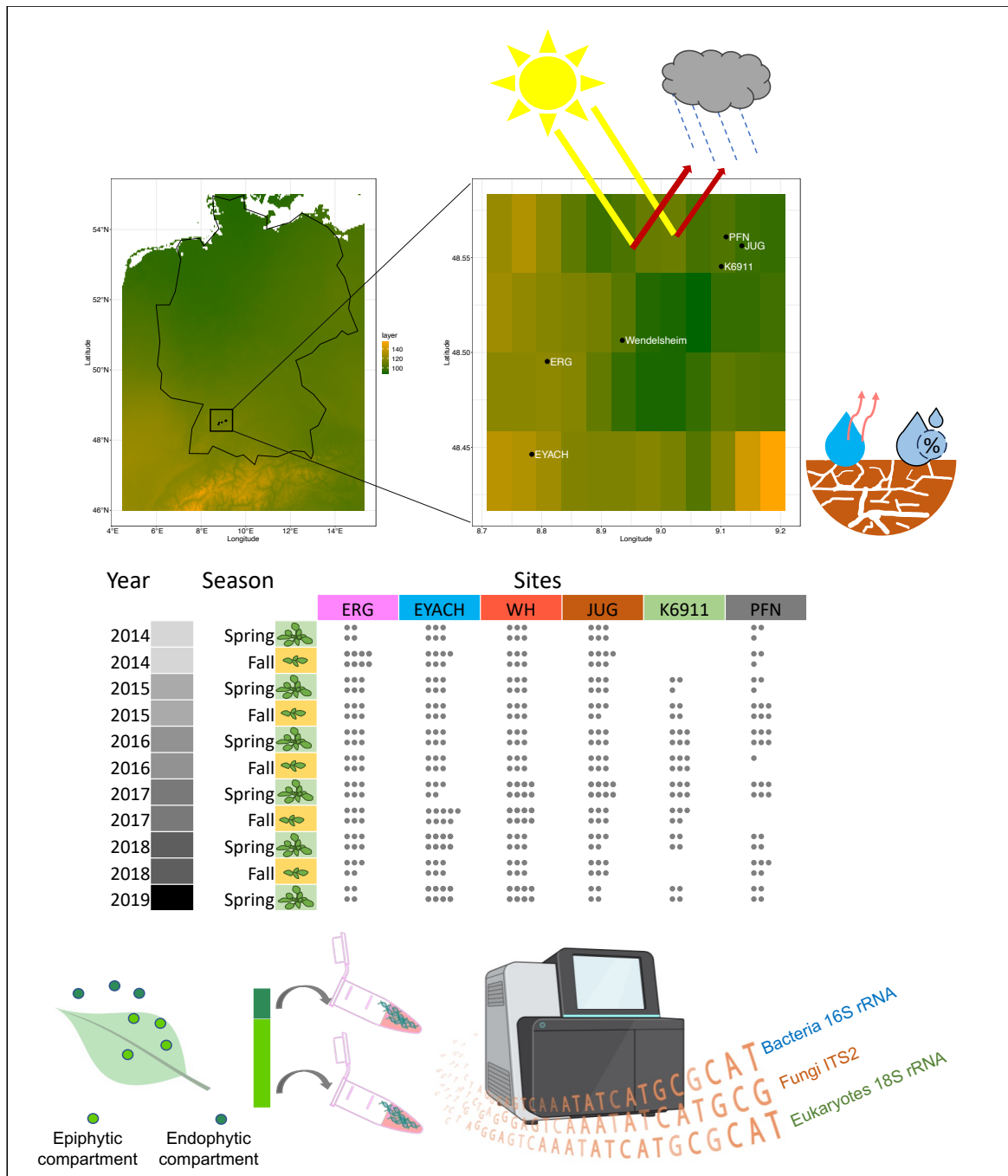


Figure 1. Microbial community collection in natural *A. thaliana* populations over time. Map showing the six sampling locations of natural *A. thaliana* in southern Germany near Tuebingen [27]. Heatmap of the map shows the spatial radiations. Plants were collected in fall and spring of five consecutive years (start spring 2014 to spring 2019, eleven *time* points, dots represent the sampled plants). Leaf samples were taken for microbiome analysis of epiphytic and endophytic compartments with a total number of 703 samples (see Table. S1). Microbiome analysis was conducted via Illumina-based amplicon sequencing (Miseq 2×300 cycle). Environmental variables (Table. S3) used in this study were obtained from the Terraclimate [71] database.

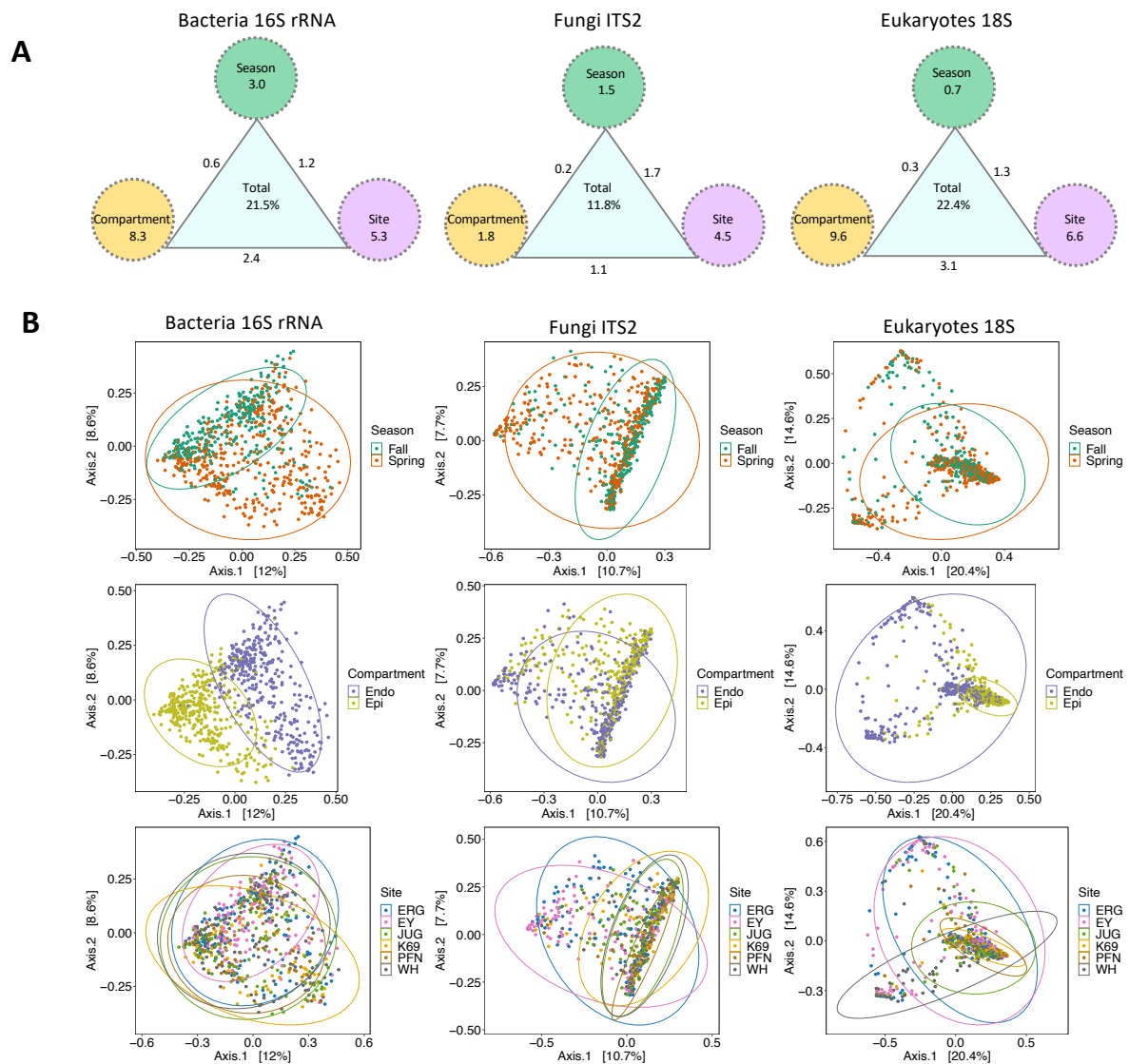


Figure 2. Multivariate analysis on factors structuring leaf microbial communities. (A) A PerMANOVA analysis on Bray-Curtis distances was conducted using the Adonis2 function in Vegan. Circles depict the percentage of variance explained by factors 'season', 'compartment' and 'site', connecting lines depict the percentage of variance explained by interactions between factors. Only significant effects are shown (permutations 10,000, $P < 0.05$, explanatory categorical variables: Season x Compartment x Site). (B) Principal coordinates analysis of epiphytic and endophytic samples of different seasons and sites, measured by principal Bray-Curtis distances in bacterial, fungal and eukaryotes communities.

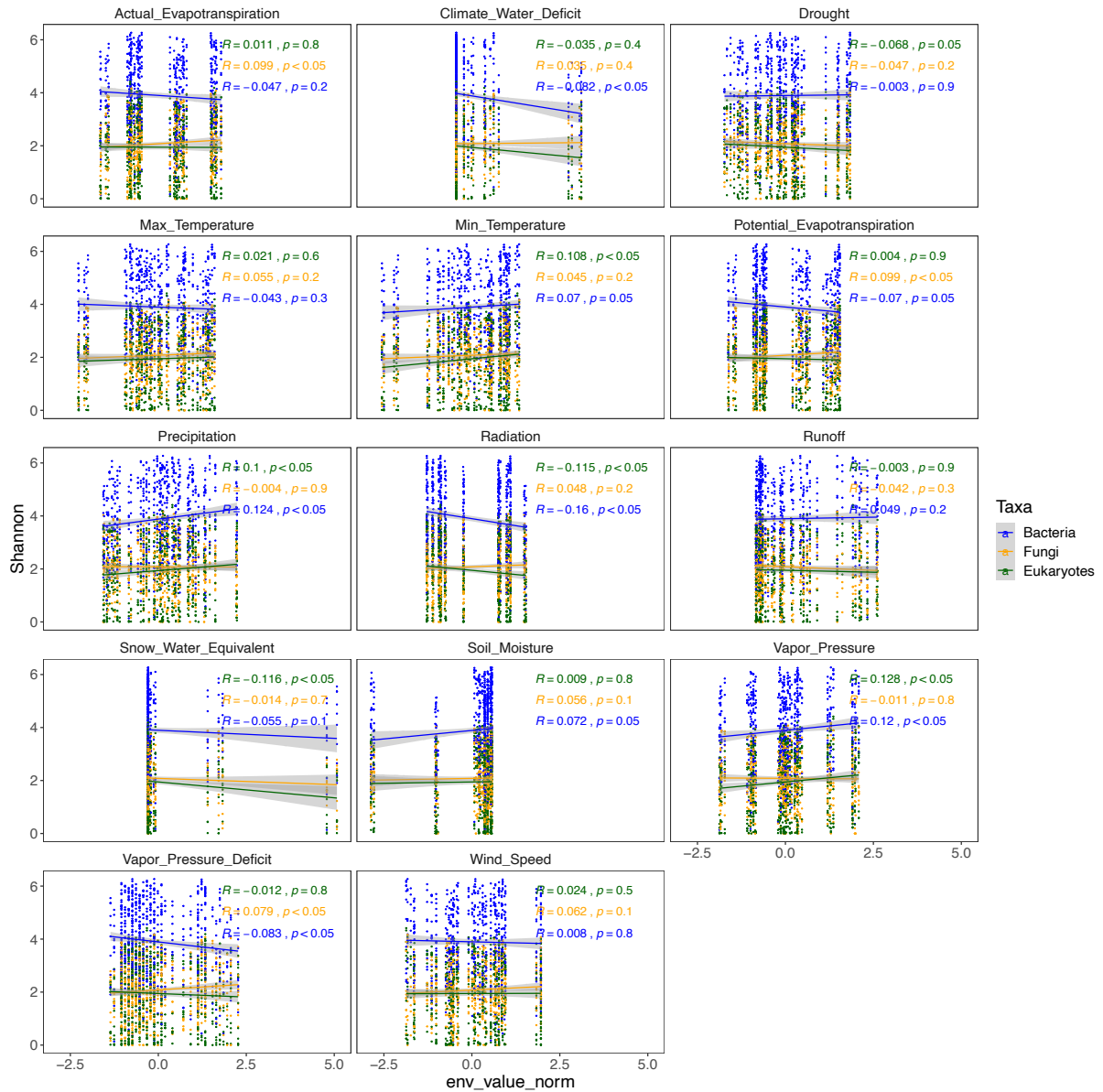


Figure 3. The relationship between alpha diversity (as measured by Shannon's H index) and various environmental factors. Each plot shows a linear regression model fit to the data, with individual samples represented by dots. The bacterial community is represented in blue, the fungal community in orange, and other eukaryote communities in a different color. Grey lines indicate 95% confidence intervals, and the Spearman correlation coefficient (R) and significant correlations ($P < 0.05$) are also shown.

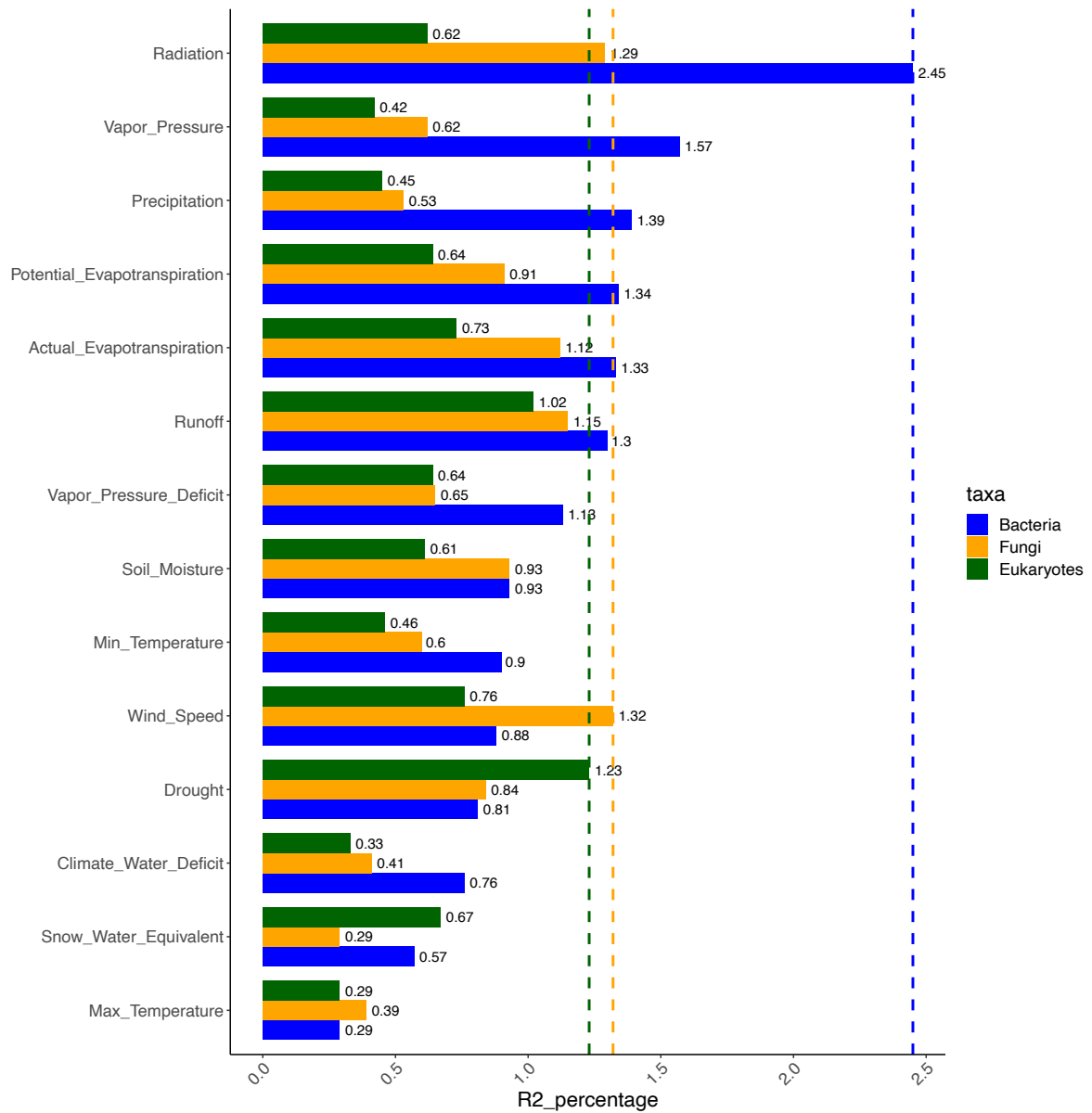


Figure 4. Permutation analysis of variance (PERMANOVA) to investigate the impact of environmental factors on the structure of leaf microbial communities. The analysis was performed using the Adonis2 function in the Vegan package, based on Bray-Curtis distances. The bar plots show the percentage of variance explained by each factor for the bacterial (blue), fungal (orange), and eukaryotes (green) communities. The highest level of explained variation for each microbial group is indicated by a vertical line.

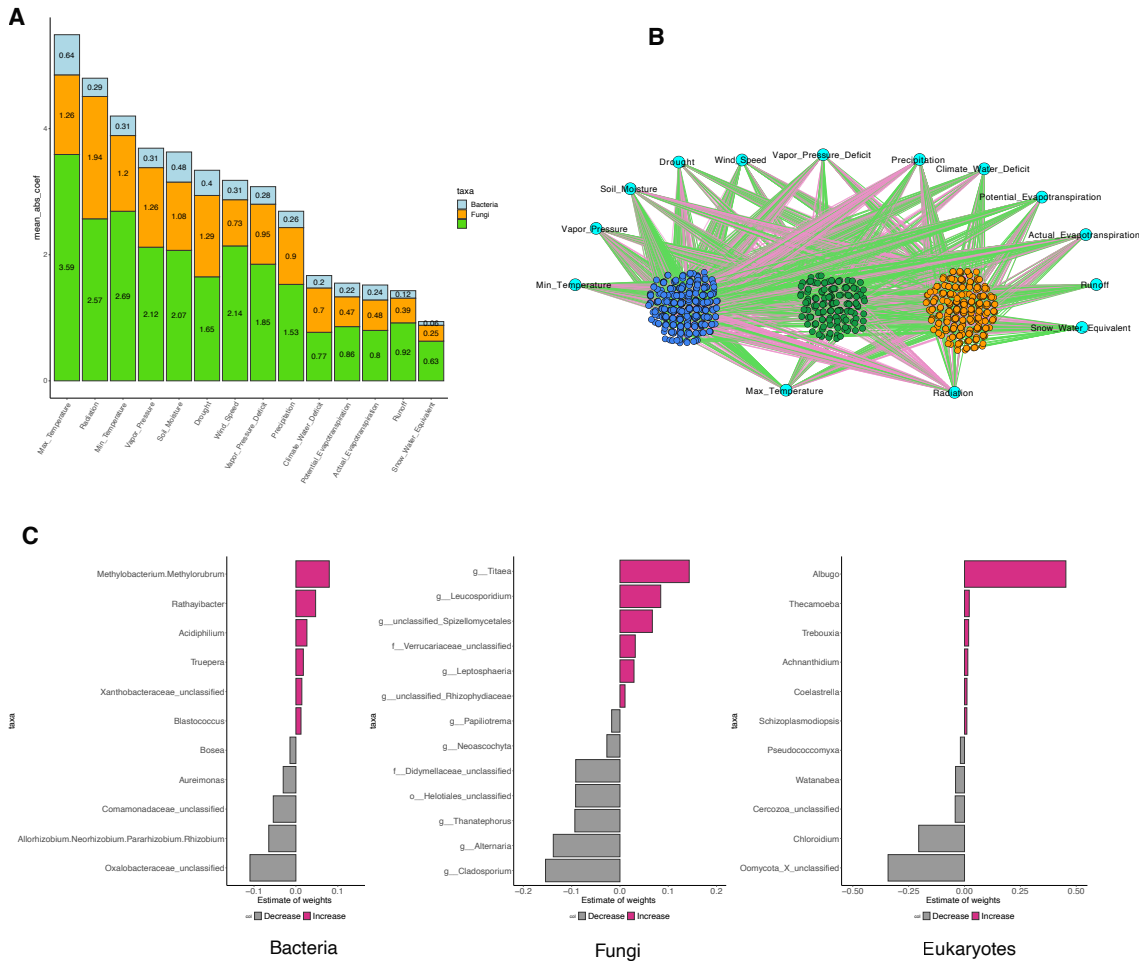


Figure 5. Demonstrates how environmental factors can predict the relative abundance of microbiome taxa. (A) The histograms in the figure represent the average of the absolute coefficient values of each environmental factor that significantly ($p < 0.05$) predicts the relative abundances of bacteria (blue), fungi (orange), and other eukaryotes (green). (B) In the figure, a network of interactions between environmental factors and the microbiome is also shown. The nodes (dots) represent environmental factors or microbes, and the edges (colored lines) depict potential positive and negative coefficient values from the linear regression model. (C) The histograms represent the coefficient values (absolute values ≥ 0.01) calculated using the linear regression model at the genus level for differentially abundant microbes according to maximum temperature in bacteria and eukaryotes, and radiation in fungi. Negative coefficient values (gray bars) represent genera that decrease with these environmental factors, while positive values (pink bars) indicate genera that increase with these factors.

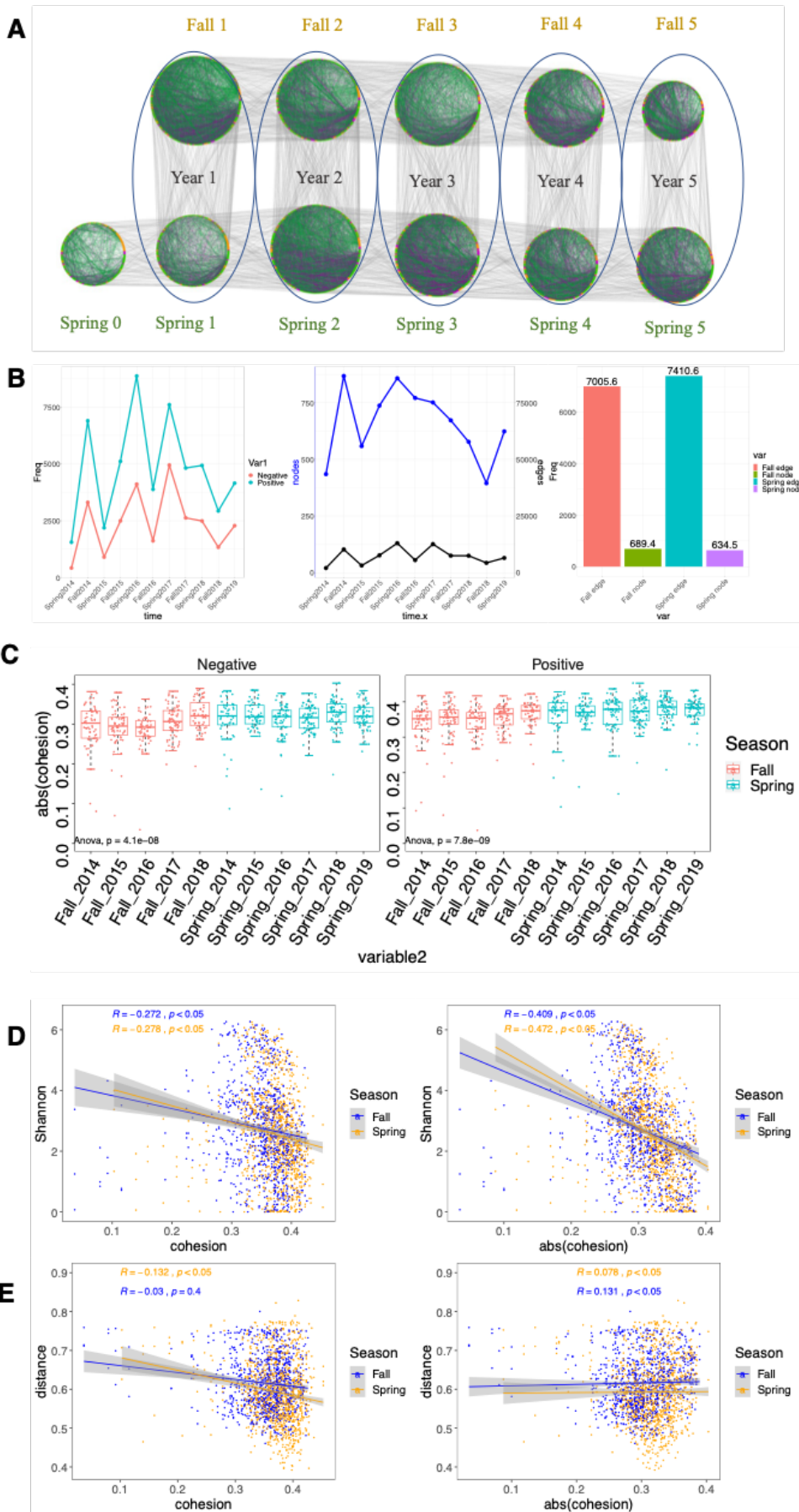
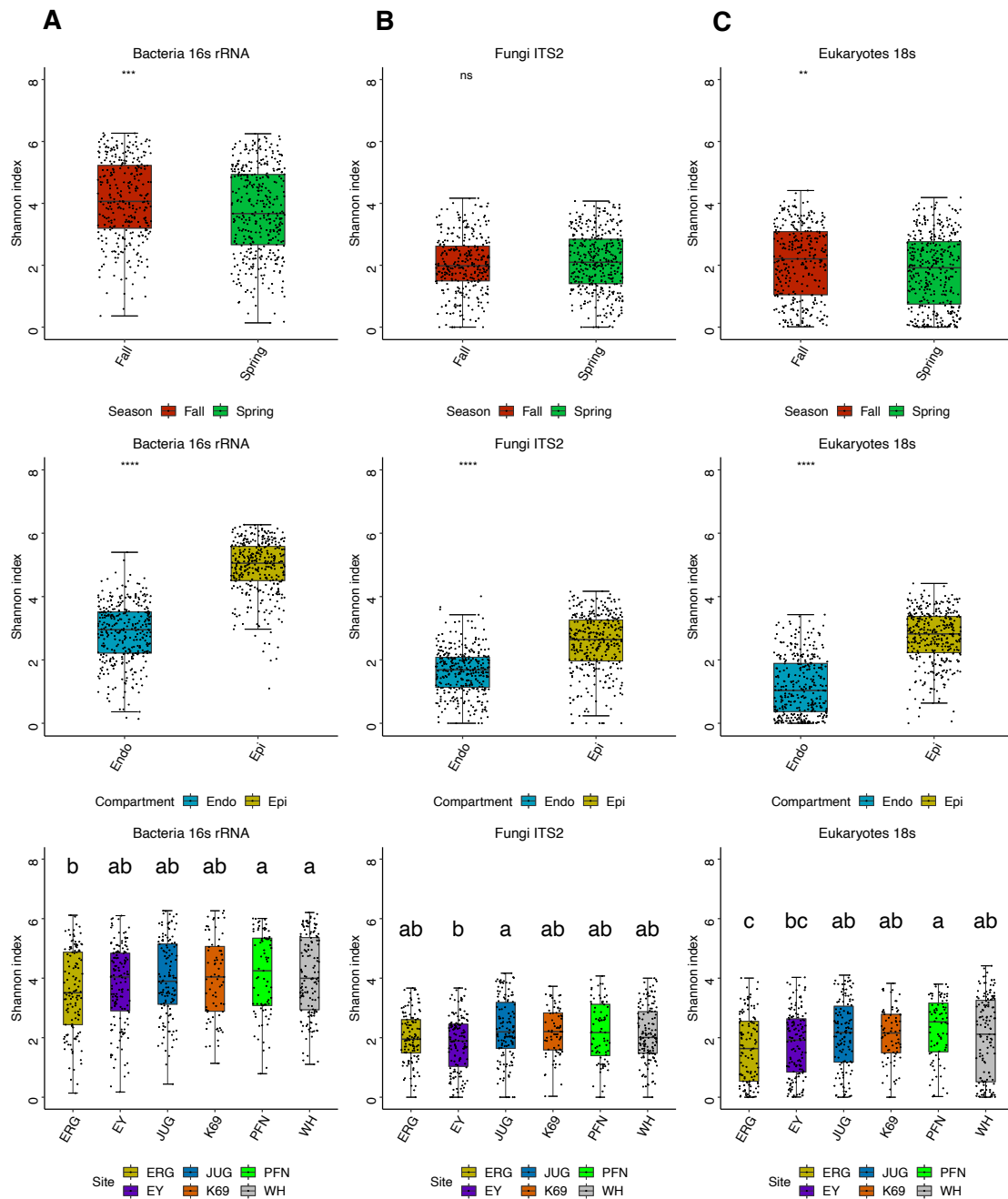
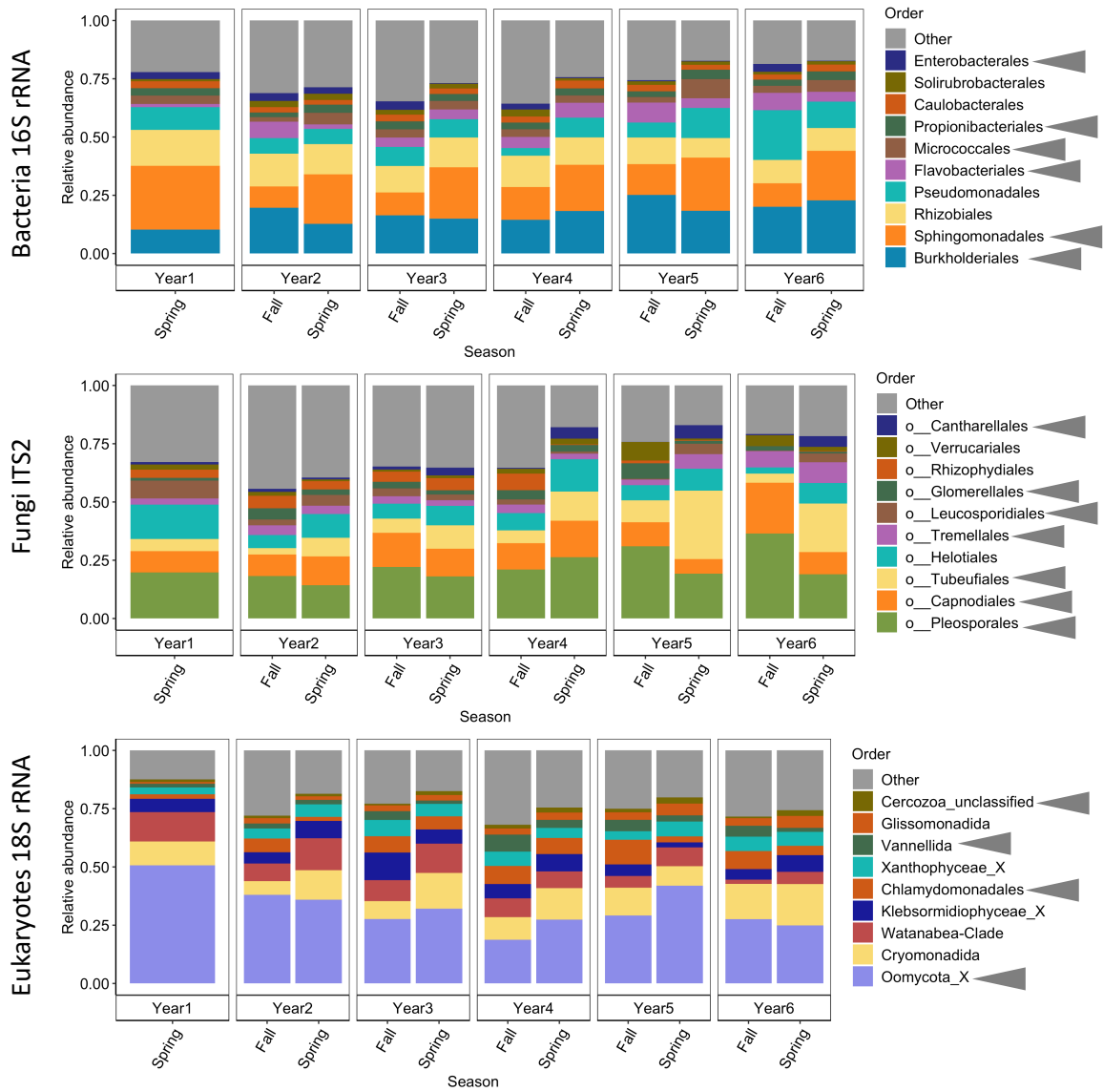


Figure 6. Changes in microbial interaction networks throughout the growing season of *A. thaliana* over multiple years. (A) Data from each time point was used to reconstruct co-abundance networks for each season using the SparCC algorithm. The nodes (dots) represent OTUs, and the edges (colored lines) depict potential positive and negative interactions between OTUs (connections). Gray lines connecting the networks show nodes that are conserved in networks from one time point to the next (inherited nodes). (B) Shows the number of nodes and edges in each time point and then the averages per season. (C) Box plots represent the negative and positive cohesions in each time point. (D) Shows the correlation between positive and negative cohesions with alpha-diversity (as measured by Shannon's H index) over seasons. (E) Shows the correlation between positive and negative cohesions and within-season variability (distance to the group centroid; beta-dispersion) over seasons. The grey lines indicate 95% confidence intervals, and the Spearman correlation coefficient (R) and significant correlations ($P < 0.05$) are also shown. Individual samples are represented by dots.

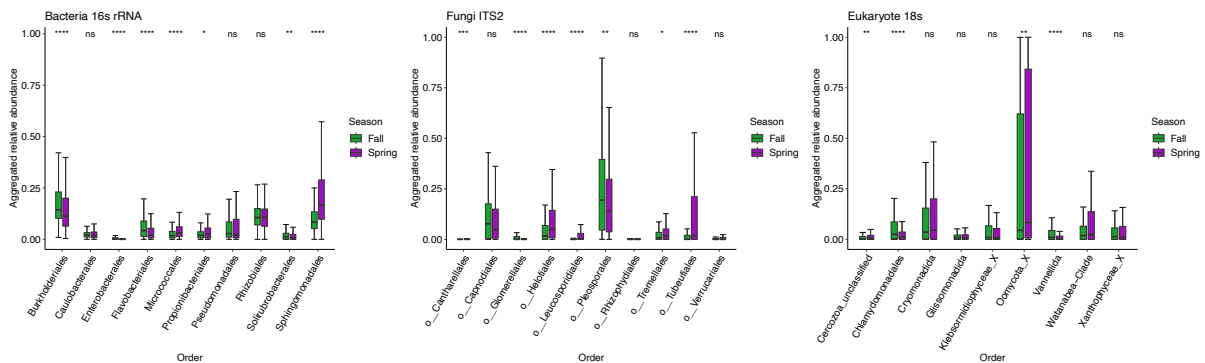
Supplementary figures legends



Supplementary figure 1. Changes in alpha-diversity of leaf microbial communities are presented in this figure, with Shannon's H index used as the diversity metric. The alpha diversity of bacteria (a), fungi (b), and other eukaryotes (c) are shown for different seasons, compartments, and sites. The box plots display individual samples as dots, with whiskers representing the dispersion of the data (1.5 x interquartile range). Significance values, based on Wilcoxon's test comparisons of alpha diversity indexes between samples, are denoted as ns ($p > 0.05$), * ($p \leq 0.05$), ** ($p \leq 0.01$), or *** ($p \leq 0.001$). Different letters indicate significant differences between groups (Dunn test, $P < 0.05$).



Supplementary figure 2 The composition of the *Arabidopsis* leaf microbiome changes throughout plant growth. The bar chart displays the aggregated relative abundance of bacteria, fungi, and other eukaryotic communities at the order level, grouped by season across five years (11 time points) for each microbial group. Arrowheads indicate taxa exhibiting marked seasonal patterns.

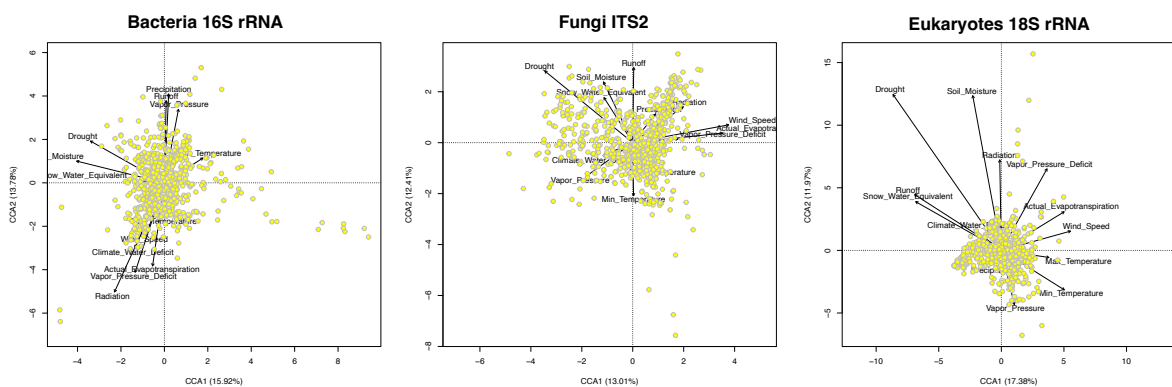


Supplementary figure 3 Seasonal changes in high abundance microbial taxa colonizing *A. thaliana*'s leaves. Boxplots show the relative abundance of the bacterial, fungal and eukaryotic orders in single samples aggregated by 'season'. Whiskers depict the dispersion of the data (1.5 x interquartile range),

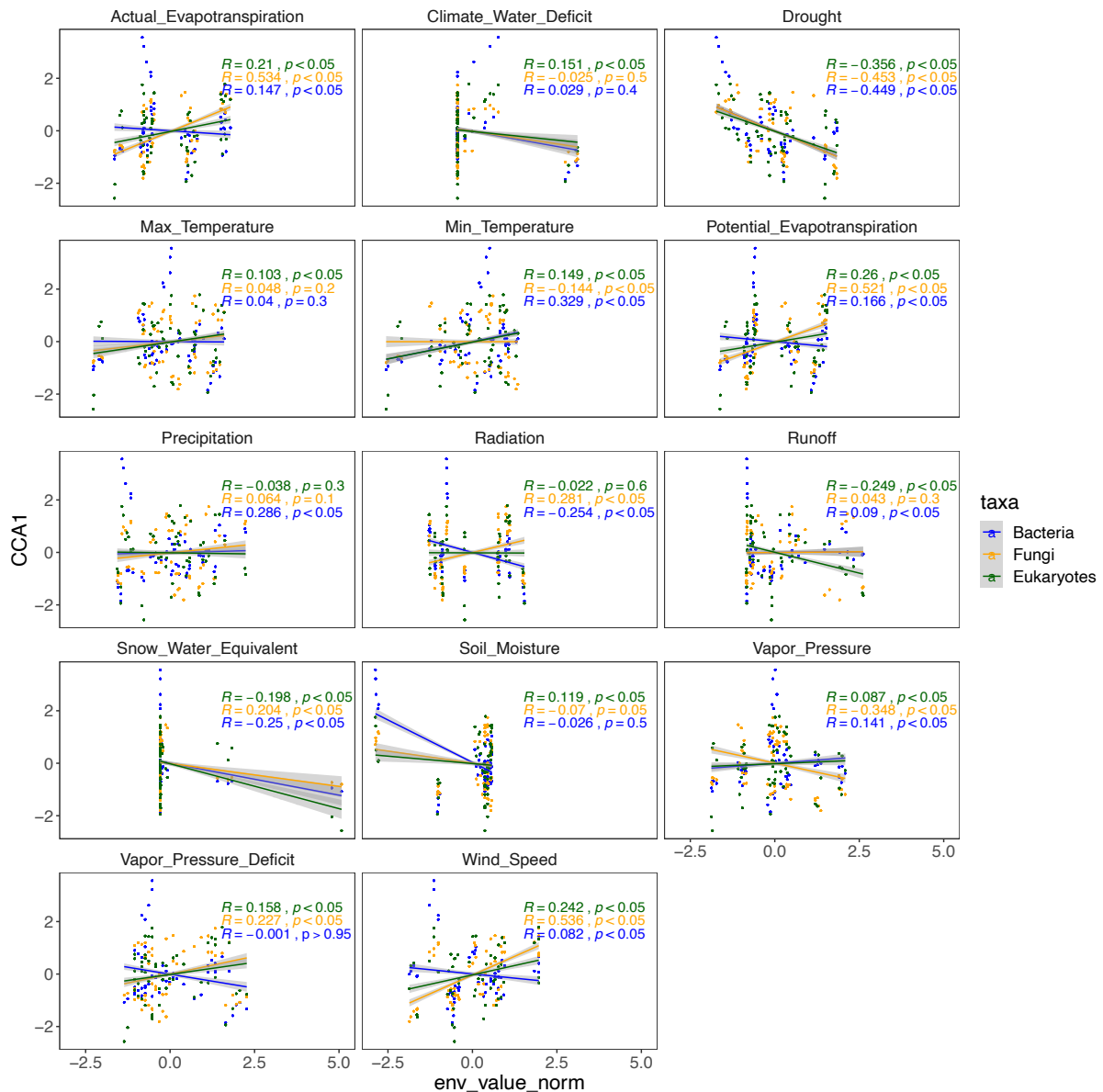
Significance values show the differences of microbes between seasons based on Wilcoxon's test (ns: p value > 0.05, *p < 0.05, **p < 0.01, ***p < 0.001).



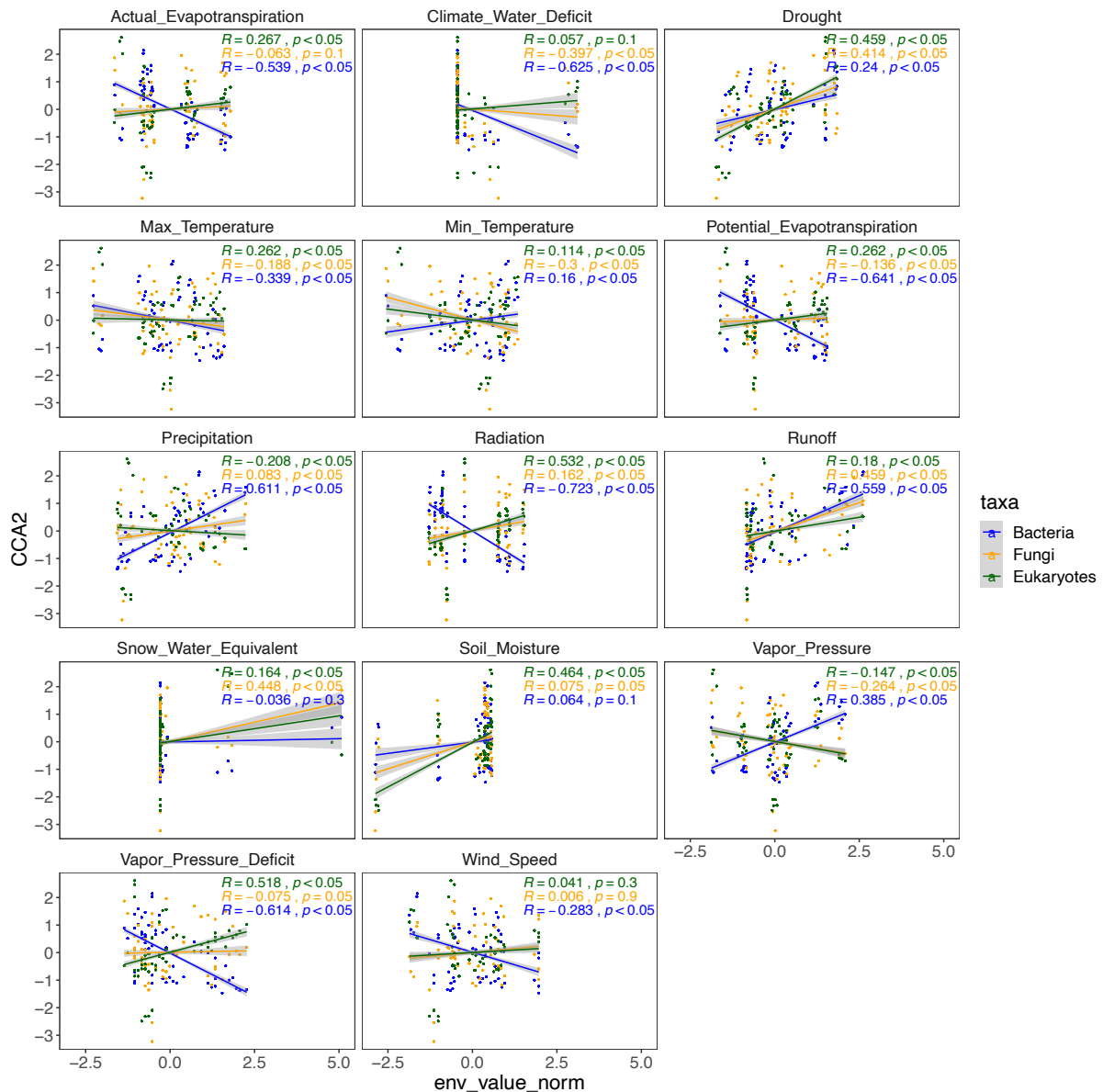
Supplementary figure 4. Environmental factors over sampling time points. (A) Lines show the average of each environmental factor for sampling month over years. (B) Box plot represents differences of average of environmental factor for sampling month in spring and fall. Significance values show the differences of environmental factors between seasons based on Wilcoxon's test (ns: p value > 0.05, *p < 0.05, **p < 0.01, *p < 0.001).**



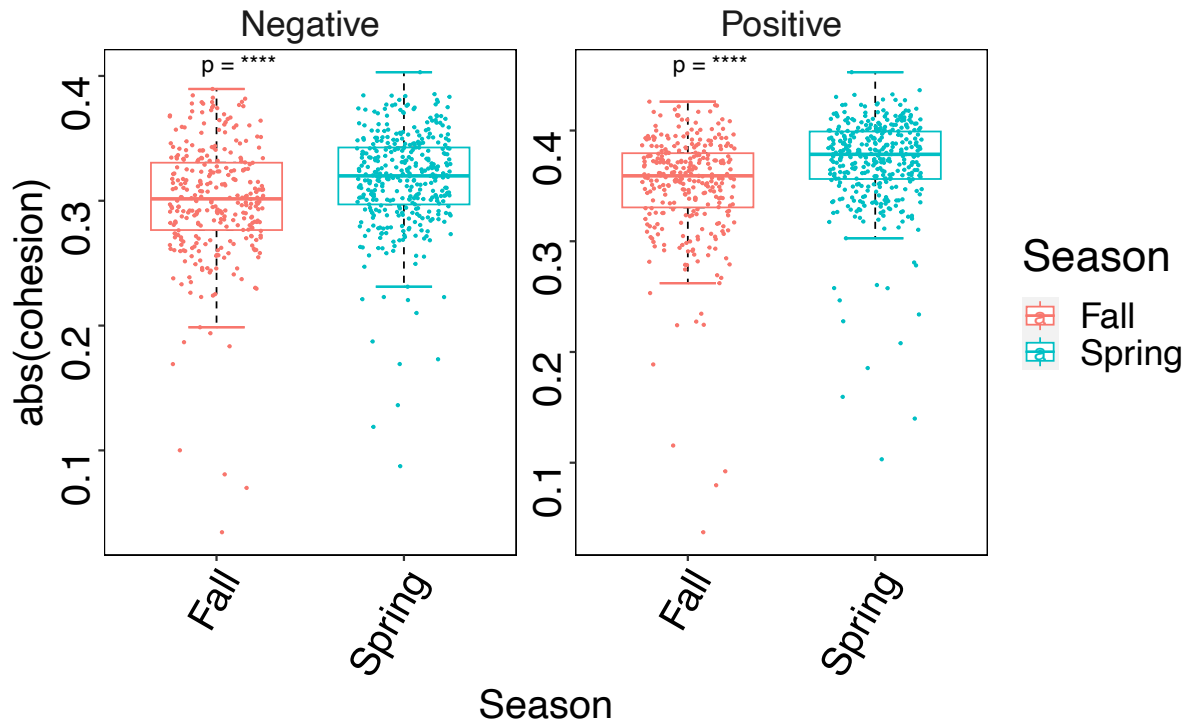
Supplementary figure 5. Canonical correspondence analysis (CCA) to examine the relationship between environmental factors and bacterial, fungal, and eukaryotic communities.



Supplementary figure 6. Canonical correspondence analysis (CCA) to examine the relationship between environmental factors and microbiome data. The plots illustrate the relationship between the first canonical correspondence axes and various environmental factors. Each plot includes a linear regression model fitted to the data, with individual samples represented by dots. The bacterial community is represented in blue, the fungal community in orange, and other eukaryote communities in green. The grey lines indicate 95% confidence intervals, while the Spearman correlation coefficient (R) and significant correlations ($P < 0.05$) are also provided.

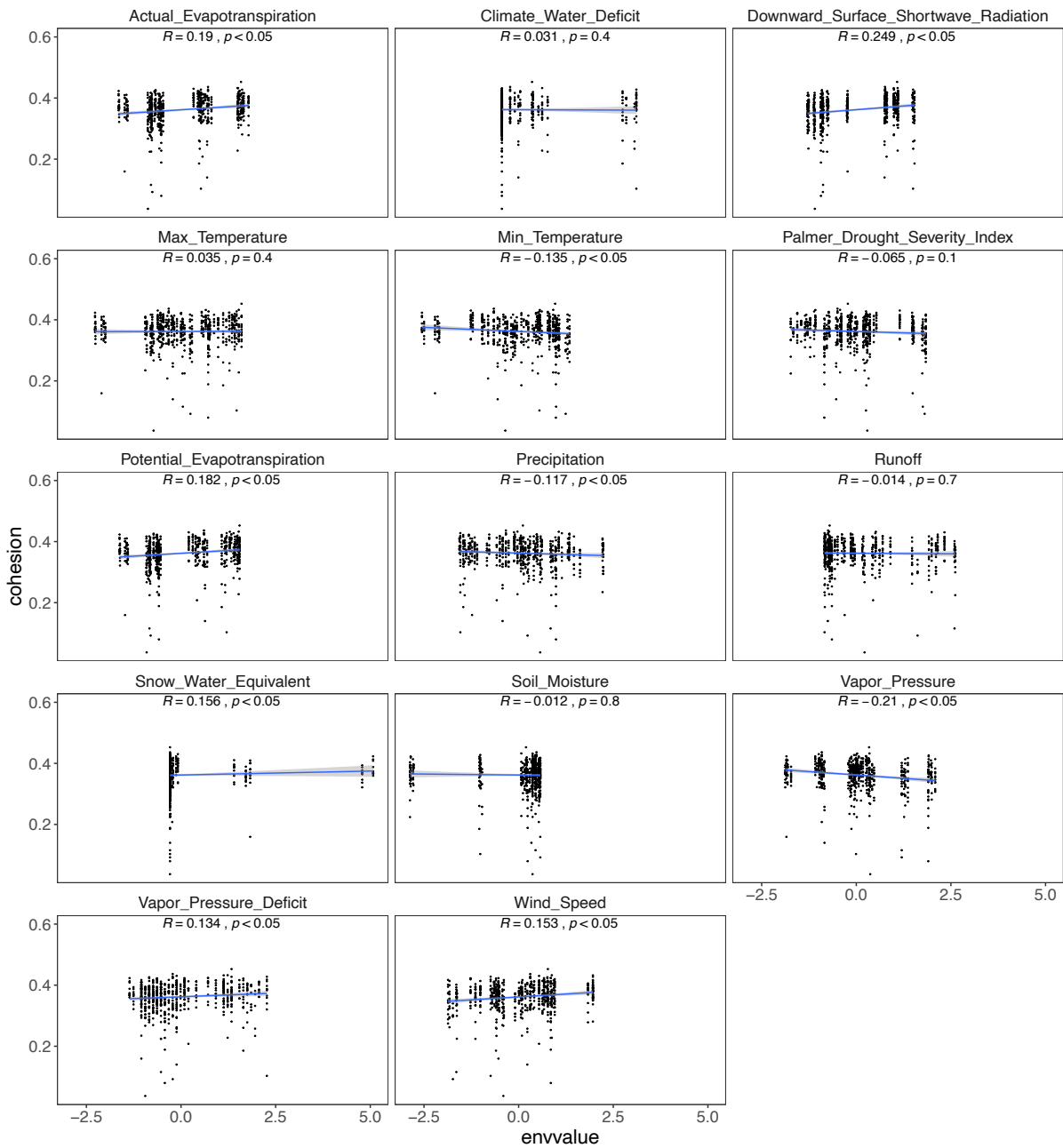


Supplementary figure 7. Canonical correspondence analysis (CCA) to examine the relationship between environmental factors and microbiome data. The plots illustrate the relationship between the second canonical correspondence axes and various environmental factors. Each plot includes a linear regression model fitted to the data, with individual samples represented by dots. The bacterial community is represented in blue, the fungal community in orange, and other eukaryote communities in green. The grey lines indicate 95% confidence intervals, while the Spearman correlation coefficient (R) and significant correlations ($P < 0.05$) are also provided.

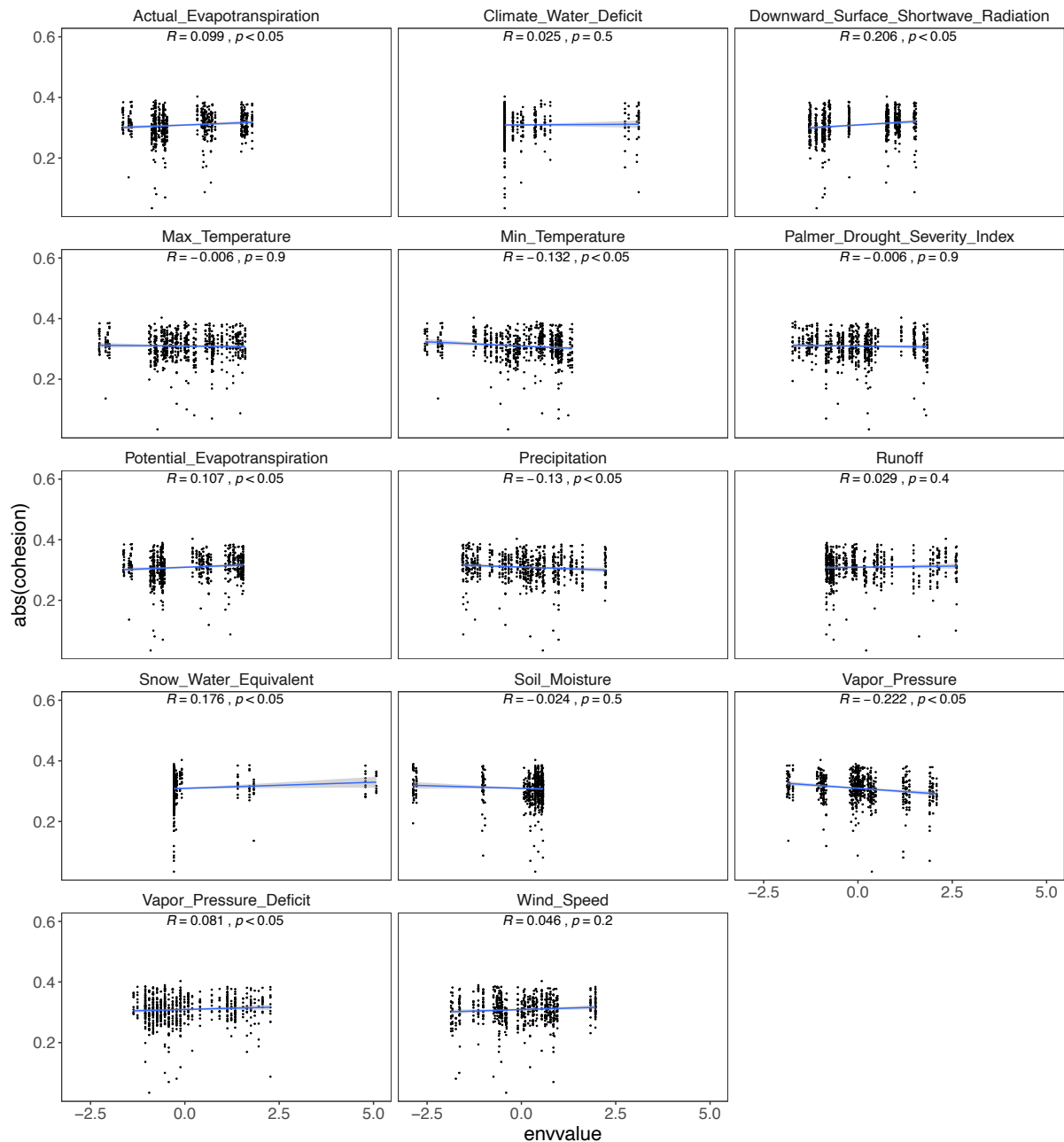


Supplementary figure 8. Box plot of the negative and positive cohesions over seasons.

Significance values, based on Wilcoxon's test comparisons of alpha diversity indexes between samples, are denoted as ns ($p > 0.05$), * ($p \leq 0.05$), ** ($p \leq 0.01$), or *** ($p \leq 0.001$).



Supplementary figure 9. The relationship between positive cohesion and various environmental factors. Each plot shows a linear regression model fit to the data, with individual samples represented by dots. Grey lines indicate 95% confidence intervals, and the Pearson correlation coefficient (R) and significant correlations ($P < 0.05$) are also shown.



Supplementary figure 10. The relationship between negative cohesion and various environmental factors. Each plot shows a linear regression model fit to the data, with individual samples represented by dots. Grey lines indicate 95% confidence intervals, and the Pearson correlation coefficient (R) and significant correlations ($P < 0.05$) are also shown.

Supplemental Material

Table S1. Experimental set-up and sampling locations. Numbers indicate sampled plants by condition.

Table S2. ANOVA results to determine the effects of the 'Site', 'Season' and 'Compartment' on microbial diversity of bacteria, fungi and eukaryotes.

Table S3. The environmental variables obtained from TerraClimate [70], a database with monthly temporal resolution and approximately 4 km spatial resolution.

Table S4. Results of PERMANOVA to investigate the impact of environmental factors on the structure of bacteria, fungi and eukaryotic communities.